AD-A049 277 NATIONAL AVIATION FACILITIES EXPERIMENTAL CENTER ATL--ETC F/G 1/4
DERIVATION OF GROUNDSPEED INFORMATION FROM AIRBORNE DISTANCE ME--ETC(U)
NOV 77 J GALLAGHER, W LYNN, R H PURSEL

UNCLASSIFIED FAA-NA-77-28 FAA-RD-77-135 NL

| OF |
AD
A049277

END
DATE
FILMED
3-78
DDC

Report No. FAA-RD-77-135

DERIVATION OF GROUNDSPEED INFORMATION FROM AIRBORNE DISTANCE MEASURING EQUIPMENT (DME) INTERROGATORS

John Gallagher
William Lynn
Robert H. Pursel

November 1977

FINAL REPORT

Prepared for

U. S. DEPARTMENT OF TRANSPORTATION
FEDERAL AVIATION ADMINISTRATION
Systems Research & Development Service
Washington, D.C. 20590

NOTICE

METRIC CONVERSION FACTORS

Approximate Conversions to Metric Measures

Symbol	When You Know	Multiply by	To Find	Symbol
		LENGTH		
in	inches	*2.5	centimeters	cm
ft	feet	30	centimeters	cm
yd	yards	0.9	meters	m
mi	miles	1.6	kilometers	km
		AREA		
in^2	square inches	6.5	square centimeters	cm^2
ft^2	square feet	0.09	square meters	m^2
yd^2	square yards	0.8	square meters	m^2
mi^2	square miles	2.6	square kilometers	km^2
	acres	0.4	hectares	ha
		MASS (weight)		
oz	ounces	28	grams	g
lb	pounds	0.45	kilograms	kg
	short tons (2000 lb)	0.9	tonnes	t
		VOLUME		
tsp	teaspoons	5	milliliters	ml
Tbsp	tablespoons	15	milliliters	ml
fl oz	fluid ounces	30	milliliters	ml
c	cups	0.24	liters	l
pt	pints	0.47	liters	l
qt	quarts	0.95	liters	l
gal	gallons	3.8	liters	l
ft^3	cubic feet	0.03	cubic meters	m^3
yd^3	cubic yards	0.76	cubic meters	m^3
		TEMPERATURE (exact)		
°F	Fahrenheit temperature	5/9 (after subtracting 32)	Celsius temperature	°C

*1 in = 2.54 (exactly). For other exact conversions and more detailed tables, see NBS Misc. Publ. 286, Units of Weights and Measures, Price $2.25, SD Catalog No. C13.10:286.

Approximate Conversions from Metric Measures

Symbol	When You Know	Multiply by	To Find	Symbol
		LENGTH		
mm	millimeters	0.04	inches	in
cm	centimeters	0.4	inches	in
m	meters	3.3	feet	ft
m	meters	1.1	yards	yd
km	kilometers	0.6	miles	mi
		AREA		
cm^2	square centimeters	0.16	square inches	in^2
m^2	square meters	1.2	square yards	yd^2
km^2	square kilometers	0.4	square miles	mi^2
ha	hectares (10,000 m^2)	2.5	acres	
		MASS (weight)		
g	grams	0.035	ounces	oz
kg	kilograms	2.2	pounds	lb
t	tonnes (1000 kg)	1.1	short tons	
		VOLUME		
ml	milliliters	0.03	fluid ounces	fl oz
l	liters	2.1	pints	pt
l	liters	1.06	quarts	qt
l	liters	0.26	gallons	gal
m^3	cubic meters	35	cubic feet	ft^3
m^3	cubic meters	1.3	cubic yards	yd^3
		TEMPERATURE (exact)		
°C	Celsius temperature	9/5 (then add 32)	Fahrenheit temperature	°F

Technical Report Documentation Page

1. Report No.	2. Government Accession No.	3. Recipient's Catalog No.
FAA-RD-77-135		

4. Title and Subtitle
DERIVATION OF GROUNDSPEED INFORMATION FROM AIRBORNE DISTANCE MEASURING EQUIPMENT (DME) INTERROGATORS.

5. Report Date
November 1977

6. Performing Organization Code

7. Author(s)
John Gallagher, William Lynn, and Robert H. Pursel

8. Performing Organization Report No.
FAA-NA-77-28

9. Performing Organization Name and Address
Federal Aviation Administration
National Aviation Facilities Experimental Center
Atlantic City, New Jersey 08405

10. Work Unit No. (TRAIS)

11. Contract or Grant No.
073-320-100

12. Sponsoring Agency Name and Address
U.S. Department of Transportation
Federal Aviation Administration
Systems Research and Development Service
Washington, D.C. 20590

13. Type of Report and Period Covered
Final rept.
October 1975-September 1976

14. Sponsoring Agency Code

15. Supplementary Notes
56p.

16. Abstract

Laboratory and flight tests were conducted to investigate the derivation of aircraft groundspeed from the range rate pulse information obtained from ARINC 568 distance measuring equipment (DME) interrogators. Initial tests determined the limitation of the range rate pulse output from the two interrogaters tested. Subsequent effort was directed toward digital filtering techniques to improve accuracy and response time of the DME-derived groundspeed. Best results were obtained with either accelerometer complementation or Kalman filtering with velocity and acceleration observations. Both techniques achieved standard deviations of about 3 knots when compared to Inertial Navigation System (INS) groundspeed.

17. Key Words	18. Distribution Statement
Groundspeed Wind shear DME	Document is available to the public through the National Technical Information Service, Springfield, Virginia 22151

19. Security Classif. (of this report)	20. Security Classif. (of this page)	21. No. of Pages	22. Price
Unclassified	Unclassified	67	

Form DOT F 1700.7 (8-72) Reproduction of completed page authorized

TABLE OF CONTENTS

LIST OF ILLUSTRATIONS

LIST OF ILLUSTRATIONS (Continued)

LIST OF ILLUSTRATIONS (Continued)

LIST OF TABLES

INTRODUCTION

PURPOSE.

The purpose of these tests was to investigate the feasibility and accuracy of deriving groundspeed information from terminal distance measuring equipment (DME).

BACKGROUND.

The potential hazards of terminal area wind shear have been brought to the attention of the aviation community by several recent accidents. The Federal Aviation Administration (FAA) has responded by instituting an intensive program which encompasses all facets of the wind shear problem. This program is examining methods of detecting wind shear and alerting the aviation community to its presence. The detection program involves various meteorological forecasting techniques, ground detection, and airborne detection systems. This document focuses on one proposed method for developing an airborne wind shear detection system. Simulator studies and practical experience have shown that a comparison between groundspeed and airspeed can be effectively utilized to detect and counter wind shear. The problem is to determine groundspeed cheaply, accurately, and with little time lag. This report focuses on this problem.

DESCRIPTION OF EQUIPMENT.

All of the tests described in this report were done with DME interrogators conforming to Aeronautical Radio Incorporated (ARINC) specification 568. The two interrogators used were a Collins Radio 860E-3 and a King Radio KDM-7000. The ARINC 568 characteristic for the range rate output on these units is one pulse every time the aircraft distance changes by 0.01 nautical mile (nmi).

LABORATORY TEST PHASE

DISCUSSION.

Laboratory tests were accomplished on both interrogators to investigate their range rate accuracy and their response time to changes in velocity. A block diagram of the test setup is shown in figure 1. The DME under test was connected to a Squak/Naut 1 DME test set. This unit produces DME interrogation replies with various time delays to simulate aircraft distance to the DME ground transmitter. The test set can increment or decrement distance to simulate velocity and can increment or decrement velocity to simulate acceleration or deceleration.

The range rate ouput pulse spacing was measured by a frequency counter and printed on a digital printer. The measurement-print cycle was synchronized to a 1-hertz (Hz) rate by a time code generator. A Hewlett-Packard 9830A calculator was programmed to convert the pulse spacing measurements to velocity data and graph the results.

TEST PROCEDURES.

Four series of tests were conducted. In the first, the velocity was smoothly incremented or decremented by 5 knots at a 1 foot per second squared (ft/s^2) rate. In the second series, the velocity was changed by 15 knots, at 1 ft/s^2. In the third series, the velocity was changed instantaneously by 5 knots. In the fourth series, the velocity was changed instantaneously by 15 knots. In all tests the interrogators were allowed to lock on and stabilize at constant velocity for approximately 5 minutes before any variations were introduced.

The King KDM-7000 was operated in both a high pulse repetition frequency (PRF) mode of 72 pulses per second (pps) and its normal PRF of 12 pps. A minor internal modification consisting of one jumper was necessary to allow the King KDM-7000 interrogator to operate in the higher PRF mode. The Collins 860E-3 did not have the high PRF capability and therefore was operated only in its normal PRF mode which was 18 pps.

TEST RESULTS.

The range rate output of the Collins 860E-3 is reasonably stable and accurate but slow to respond to changes in velocity. Figures 2 and 3 illustrate range rate responses for velocity changes of -5 and -15 knots. The velocity change from the test set to the interrogator was accomplished at a rate of 1 ft/s^2.

The interrogators were also subjected to step inputs from the test set. Figures 4 and 5 illustrate the response of the 860E-3 range rate output to step inputs of -5 and -15, respectively. The interrogator was also subjected to increasing velocity rates and step changes. The results were similar to those shown for the decreasing rates and step changes.

Similar tests were conducted on the King KDM-7000 interrogator, but it quickly became evident that the range rate output was extremely noisy. Figure 6 illustrates the range rate output for a constant velocity of 120 knots. In order to produce a discernable plot, a smoothing calculation was performed by taking an equal-weighted average of 10 preceding points (including the data point in question) and then plotting this value. This technique was used to produce the plot of figure 7 which represents the filtered output of the King interrogator subjected to a velocity change of -15 knots. Statistics were run on the error between the range rate outputs of both interrogators and a constant velocity input from the test set. The error was determined from the equation: Error = Measured Groundspeed - Input Reference Groundspeed. The statistics are presented in table 1.

TABLE 1. STATISTICAL ERROR TABULATION OF CONSTANT VELOCITY LABORATORY TEST RESULTS FOR COLLINS AND KING INTERROGATORS

Interrogator	Number of Samples	Mean Error (knots)	Standard Deviation (knots)
860E-3	100	-1.25	1.15
KDM-7000	100	1.54	19.30

Statistics were also generated for the King KDM-7000 for the two different PRF's at which it was capable of operating. These statistics are presented in table 2. The samples were taken at a constant velocity of 120 knots.

TABLE 2. STATISTICAL ERROR TABULATION OF CONSTANT VELOCITY LABORATORY TEST RESULTS FOR KING INTERROGATOR AT LOW AND HIGH PRF's

PRF (pps)	Number of Samples	Standard Deviation (knots)
12	50	17.5
72	50	20.1

PRELIMINARY FLIGHT TEST PHASE

DISCUSSION.

The test setup used in the aircraft, a Grumman Gulfstream I, was identical to the setup used in the laboratory, with the exception that the DME test set was not required. All data runs were approaches to the National Aviation Facilities Experimental Center (NAFEC) runway 13, using the commissioned instrument landing system (ILS) and terminal DME.

The terminal DME used in these tests was a Butler National Corporation Model 1020. This is a low-powered (90 watt (W) nominal) DME designed for terminal use. This equipment had been previously evaluated at NAFEC on other programs. Reports issued on it include, "Test and Evaluation of Engineering Models of Terminal Area DME," FAA-RD-71-108, by George J. Hartranft and "Evaluation of Techniques Used in the Butler Terminal Area Model 1020 Distance Measuring Equipment," FAA-RD-74-208, by Robert H. Erikson.

The first series of approaches were tracked by the NAFEC photo-optical theodolite system, while the second series of approaches were tracked by the Extended Area Instrumentation Radar (EAIR). The data from these tracking facilities provided the groundspeed reference against which the DME-derived groundspeed was compared.

TEST PROCEDURES.

The first series of approaches focused on the time delays involved in sensing a change of velocity due to aircraft acceleration or deceleration. On the approach, the aircraft stabilized at constant airspeed for at least 2 minutes, then accelerated or decelerated from 125 to 140 knots true airspeed (TAS) or vice versa. This final speed was held until threshold, approximately 2 more minutes. Eight runs were flown this way, four recording the output of the KDM-7000 interrogator, and four recording the output of the 860E-3 interrogator.

The KDM-7000 was operated in the ILS mode with an interrogation rate of 72 pps. The 860E-3 does not have a high-PRF mode and was operated at the normal PRF of 18 pps. The second series of approaches were flown at as constant an airspeed as could be maintained during the approach.

TEST RESULTS.

Figures 8 and 9 show typical results from the two interrogators on acceleration/deceleration runs. Collins 860E-3 range rate outputs are typified by figure 8, which represents an acceleration of about 15 knots. Phototheodolite tracking provides the groundspeed reference. The time lag in the response of the 860E-3 is evident. No statistical calculations were made, because the standard deviation of the tracking data was higher than that of the DME range rate data.

The range rate outputs of the King KDM-7000 are typified by figure 9, which represents a deceleration of about 15 to 20 knots. EAIR tracking provides the groundspeed reference. The noisy response is evident. The flight test data on the King interrogator agrees closely with laboratory test data. Typical test data resulted in a mean error of -4.0 knots and a standard deviation of 19.2 knots for 102 samples.

SUMMARY OF LABORATORY AND PRELIMINARY FLIGHT TEST RESULTS.

The results of the preliminary flight tests as well as the laboratory tests are summarized in table 3. This data summary makes it obvious that the range rate outputs of these two interrogators are not usable in their present form to provide groundspeed input to a wind shear detection algorithm. Further processing of the range rate outputs of either DME is required to produce usable groundspeed.

TABLE 3. SUMMARY OF LABORATORY AND PRELIMINARY FLIGHT TEST RESULTS FOR COLLINS AND KING INTERROGATORS

	Collins 860E-3	King KDM-7000
Range Rate Delay	30-45 second delay	very little delay
Constant Velocity Mean Error	within 1.5 knots	within 2.0 knots
Constant Velocity Standard Deviation	±1.2 knots	±20.0 knots
Usability	Range rate output not responsive enough for wind shear determination in present form.	Range rate output too noisy for wind shear determination in present form.

SUBSEQUENT FLIGHT TEST PHASE

DISCUSSION.

The results of the laboratory tests and the preliminary flight tests indicated that some sort of signal processing would be necessary in order to obtain usable, responsive, groundspeed information from either DME. Subsequently, work proceeded on determining what type of signal processing was necessary to provide usable groundspeed. This work was done as both a contractual and in-house effort.

Rockwell International, Collins Radio Group, performed some simulation work under modification two of contract DOT-FA75NA-2134. This work was done by Mr. James A. Klein of Collins Radio with assistance from Mr. David Lawrence of NAFEC. The simulation and study effort concentrated on the differential between airspeed and groundspeed as a means to detect wind shear.

Since wind shear is a very rapidly changing phenomenon, considerable time was spent during the Collins study to evaluate the amount of sensor lag on groundspeed that could be tolerated in the wind shear detection program. It was determined that groundspeed sensor lags on the order of 3 to 5 seconds yield promising results in shear detection algorithms. Accordingly, Collins developed two methods for deriving groundspeed from a 30-second-lagged DME range rate output (the 30-second-lagged DME range rate output is typical for the Collins 860E-3 interrogator).

The first method employed a lead/lag compensator to reduce the lag in DME range rate. The second method consisted of complementary lagged DME range rate with filtered, pitch-compensated, longitudinal acceleration to reduce the lag. Both of these methods were designed specifically for the 860E-3 interrogator.

In addition to these contractor-designed filters, other filter designs were developed in-house for both the Collins and King interrogators. The filter techniques considered included (1) simple low pass, (2) rate limiters plus low pass, (3) low pass plus lead/lag, (4) low pass plus accelerometer complementation, and (5) Kalman and higher order complementation. Initial findings showed several of these to be totally impractical. Therefore, only the low pass plus lead/lag, the low pass plus accelerometer complementation, and the Kalman techniques were fully developed.

All flight tests of these filter algorithms were conducted in an FAA test bed aircraft, a Convair 880. This aircraft is equipped with a Digital Equipment Corporation PDP 11/05 general purpose digital computer (figure 10). All filter algorithms were coded in BASIC software and were implemented in the digital domain on the PDP-11/05. The filter algorithms were transformed from the analog domain to the discrete-time (digital) domain by means of a bilinear Z transformation.

$$S \rightarrow \frac{2}{T} \frac{1-Z^{-1}}{1+Z^{-1}},$$

$$W_D = \frac{2}{T} \text{ Tan } \frac{W_A T}{2}$$

Where:

T = Sampling Interval
W_D = Prewarped Digital Frequency (radians/second)
W_A = Analog Frequency (radians/second)

This provided linear recursive difference equations which were easily implemented in software. The accuracy can be improved by increasing the sampling rate, the error being dependent on iterations performed as well as biasing of the analog frequency spectrum. Hardware considerations, recording capability, and simulation expectations, as well as accuracy requirements, dictated the 10-Hz sampling rate.

In addition to the general purpose digital computer, the aircraft was equipped with an aircraft systems coupler and patch panel and a NAFEC-designed and fabricated DME data interface. The aircraft systems coupler and patch panel allows various aircraft signals to be selected and applied to digital conversion circuitry with discrete UNIBUS® addresses (UNIBUS is a registered trademark of Digital Equipment Corporation). This allows the data to be addressed by the PDP 11/05 and used in the computational process. Accelerometer and vertical gyro information were input to the PDP 11/05 in this way.

The DME data interface (see block diagram figure 11) allowed the DME pulse-spacing data to be input on discrete addresses to the PDP 11/05 via the UNIBUS. The interface therefore provided all the necessary raw data to the PDP 11/05 UNIBUS.

Four UNIBUS addresses were also output to a digital data recording system. This allowed the inputs to and the outputs from the filter algorithm to be recorded. Other aircraft parameter data including inertial navigation sensor outputs were also recorded. The groundspeed output of the Inertial Navigation System, a Litton Industries LTN-51, provided the measurement reference for all of the tests in the Convair 880.

By using a ground-based PDP 11/15 general purpose computer and the digital data tape recorded on the test flight, the test approaches could be rerun on the ground and the filter algorithms modified or changed to improve performance. This reduced the number of flight hours necessary to an absolute minimum. After the algorithms were optimized on the ground-based, general purpose computer system, they were again flown in the Convair 880 to verify performance.

TEST PROCEDURES.

The filter algorithms, coded in BASIC, were loaded into the aircraft PDP 11/05 computer utilizing a high-speed paper tape reader. This procedure was repeated each time a different algorithm was to be evaluated. The computer was then placed in a run status as the aircraft turned on final approach. The aircraft was stabilized on final approach course approximately 4 nmi outside the outer marker.

Aircraft velocity was varied rapidly about the reference approach speed (approximately 135 knots) on some runs, while on other runs the changes in velocity were made slowly. Long-term accuracy and stability of the derived groundspeeds were also checked with constant speed approach runs.

TEST RESULTS.

LEAD/LAG FILTER. The contractor-designed algorithm was implemented in BASIC software and was tried using the range rate outputs of the Collins 860E-3. The algorithm was designed to reduce the inherent 30-second lag in the range rate output of this interrogator. The filter is described in block diagram form in figure 12.

Raw DME range rate data are plotted along with the reference Inertial Navigation System (INS) groundspeed in figure 13. In this run, aircraft speed was slowly varied about a reference speed. The effects of the internal filtering of the 860E-3 can be seen in the lack of responsiveness of the DME range rate output to the changes in groundspeed.

Figure 14 is a plot of the output of the lead/lag filter along with the reference INS groundspeed for an 860E-3 data run with slowly varying groundspeed. As can be seen, the output of the lead/lag filter is extremely noisy. This output was typical for other data runs with lead/lag compensation. Examination of the data shown in figure 15 can explain the problem. The two columns of figures are the raw range rate output from the interface unit and the output from the lead/lag filter. The data rate is 10 Hz. The arrows on figure 15 indicate where the raw range rate (input to the lead/lag filter) changes. In some cases, the change approaches 1 ft/s in magnitude. Since the lead/lag filter has an initial gain of 30, a 1-ft/s change on the input to the filter is seen as a 30-ft/s change on the output, thus causing the noise spikes seen in figure 14.

The problem could be minimized by increasing the range rate resolution of the DME and increasing the digital filter sampling frequency so that the input to the filter more closely approximates a continuous function.

Another solution to the problem was attempted by placing a digital low-pass filter on the range rate output of the interface unit to filter the data before processing in the digital lead/lag filter. This has the effect of approximating a continuous function input to the lead/lag filter. One negative effect of this is the introduction of a time lag on the filter output. Figure 16 shows the results of a 5-second low-pass prefilter plus the lead/lag filtration.

The data are again plotted with INS reference groundspeed and are the same data used for figure 15. The effects of the 5-second lag can be seen.

Low-pass prefilter time constants of from 2 to 10 seconds were tried on the data with 5 seconds providing the optimum statistical results. A statistical error summary of the three runs for the raw, lead/lag, and prefiltered lead/lag DME range rate data is presented in table 4. The error is calculated from the formula: Error = Measured Groundspeed - INS Reference Groundspeed.

TABLE 4. STATISTICAL ERROR SUMMARY OF RESULTS FOR LEAD/LAG FILTER COMPENSATION ON COLLINS INTERROGATOR

STABLE GROUNDSPEED

	Number of Samples	Mean Error (ft/s)	Mean Error (knots)	Standard Deviation (ft/s)	Standard Deviation (knots)
Raw	1,544	2.3	1.4	6.9	4.1
Lead/lag 5-second	1,544	4.5	2.7	28.7	17.0
Prefilter plus lead/lag	1,547	0.5	0.3	7.6	4.5

SLOWLY VARYING GROUNDSPEED

	Number of Samples	Mean Error (ft/s)	Mean Error (knots)	Standard Deviation (ft/s)	Standard Deviation (knots)
Raw	1,500	6.1	3.6	10.0	5.9
Lead/lag 5-second	1,499	5.9	3.5	23.2	13.7
Prefilter plus lead/lag	1,500	4.8	2.8	8.4	5.0

RAPIDLY VARYING GROUNDSPEED

	Number of Samples	Mean Error (ft/s)	Mean Error (knots)	Standard Deviation (ft/s)	Standard Deviation (knots)
Raw	1,499	3.6	2.1	15.8	9.4
Lead/lag 5-second	1,496	8.4	5.0	28.5	16.9
Prefilter plus lead/lag	1,499	3.2	1.9	11.5	6.8

ACCELEROMETER COMPLEMENTATION. The technique for accelerometer complementation as proposed by the contractor to reduce the lag in DME range rate is shown in block diagram form in figure 17. This technique calls for filtering pitch-compensated longitudinal acceleration with a 30-second low-pass filter which has a gain of 30. This acceleration term is added to the 30-second-lagged DME range to produce responsive groundspeed.

The accelerometer complementation algorithm was implemented in the digital domain for operation in the airborne environment on the Convair 880 and on the ground using flight test data. Initial tests yield results which were promising but in need of refinement. Figures 18, 19, and 20 illustrate the results of the initial attempts at acceleration complementation. The data runs used are for stable, slowly varying, and rapidly varying groundspeeds, respectively. The slowly varying data run is the same as was used for the lead/lag filter illustration.

As can be seen in figures 18, 19, and 20, the accelerometer-complemented groundspeed is responsive and closely follows the INS groundspeed, but is biased above the INS groundspeed. This is caused by the fact that the complementation filter exhibits a direct current (d.c.) gain of 30, so that any offset in the acceleration term will be amplified by this amount. In order to eliminate this bias effect, it is necessary to high-pass the acceleration term to wash out any d.c. component. Several factors must be taken into account in choosing the correct time constant for the high-pass filter. Considering time domain requirements, the filter should wash out in a reasonably short period of time. Frequency domain considerations require that the pole of the high-pass filter should be at least an octave below the pole of the complementary low-pass filter. These requirements are contradictory in nature.

Lowering the time constant of the high-pass filter moves its pole closer to the pole of the complementary filter. This will affect the overall gain and frequency content of the complementary acceleration to the extent that the derived groundspeed will not be able to track changes due to a sustained level of acceleration. The high-pass filter time constant should be a compromise value necessary to quickly wash out bias errors, and still pass short-term constant accelerations.

Tests showed that a 60-second filter did not hamper the responsiveness of this technique. However, the washout time was unsatisfactory, and for this reason a time-varying filter was employed. This was simple to implement as a software digital filtering algorithm.

The time constant was initialized at 1 second and incremented by 0.1 seconds per sample period until a value of 60 seconds was reached. This provided rapid initial washout of d.c. acceleration components as well as allowing the capability to track groundspeed during short term constant acceleration. Figures 21, 22, and 23 show the results obtained by prefiltering the acceleration components with a time-varying high-pass filter. The DME-derived groundspeed is very responsive. In fact, because of an approximate 2-second update rate on the INS groundspeed reference, the DME-derived groundspeed actually leads the INS groundspeed output on rapid transitions.

A similar acceleration complementation scheme was also applied to the range rate output of the King DME-7000 interrogator. It should be remembered, however, that early laboratory and flight test data showed that the range rate outputs were very noisy. This introduces a contradictory situation, in that the output must be filtered to obtain usable information, but a filtering

scheme such as a low-pass filter introduces unacceptable lags in the groundspeed output. Acceleration complementation is then needed to reduce the groundspeed lags. Figure 24 illustrates the complementation scheme eventually used for the King KDM-7000 interrogator.

Figure 25 illustrates the digitized raw range rate output of the King KDM-7000 plotted with INS groundspeed. The extremely noisy character of the range rate signal can be seen.

Figures 26, 27, and 28 illustrate the accelerometer-complemented groundspeed plotted with INS groundspeed for stable, slowly varying, and rapidly varying groundspeeds, respectively.

Some discontinuities can be seen in complemented output in figures 26, 27, and 28 (the discontinuities are circled in the figures). These are caused by instantaneous values of velocity which are far outside the expected range. The reason for these outliers is unknown, but by applying a range limiter to the raw DME range rate data (figure 29), some improvement in the output can be obtained. Figures 30, 31, and 32 illustrate the results of accelerometer complemented range rate with a range limiter on the raw range rate. The limiter restricted the raw range rate input to the filter algorithm to between 125 and 325 ft/s. Statistical summaries for the Collins and the King accelerometer-complemented range rate data are contained in tables 5 and 6, respectively. The statistics are computed starting 50 seconds after the actual start of the run to allow the high pass to settle. As can be seen from table 6, the range rate limiter does improve the statistical results of the King DME runs.

TABLE 5. STATISTICAL ERROR SUMMARY OF RESULTS FOR ACCELEROMETER COMPLEMENTATION OF COLLINS INTERROGATOR

STABLE GROUNDSPEED				
Number of Samples	Mean Error (ft/s)	Mean Error (knots)	Standard Deviation (ft/s)	Standard Deviation (knots)
1,547	2.0	1.2	4.9	2.9
SLOWLY VARYING GROUNDSPEED				
Number of Samples	Mean Error (ft/s)	Mean Error (knots)	Standard Deviation (ft/s)	Standard Deviation (knots)
1,500	8.2	4.8	6.4	3.8
RAPIDLY VARYING GROUNDSPEED				
Number of Samples	Mean Error (ft/s)	Mean Error (knots)	Standard Deviation (ft/s)	Standard Deviation (knots)
1,499	8.3	4.9	6.0	3.5

TABLE 6. STATISTICAL ERROR SUMMARY OF RESULTS FOR ACCELEROMETER COMPLEMENTATION OF KING INTERROGATOR

STABLE GROUNDSPEED

	Number of Samples	Mean Error (ft/s)	Mean Error (knots)	Standard Deviation (ft/s)	Standard Deviation (knots)
Accelerometer complemented	1,479	-1.4	-0.8	7.5	4.4
Range limited with accelerometer complementation	1,479	0.0	0.0	4.3	2.5

SLOWLY VARYING GROUNDSPEED

	Number of Samples	Mean Error (ft/s)	Mean Error (knots)	Standard Deviation (ft/s)	Standard Deviation (knots)
Accelerometer complemented	1,222	-1.7	-1.0	6.7	3.9
Range limited with accelerometer complementation	1,222	-4.0	-2.4	5.6	3.3

RAPIDLY VARYING GROUNDSPEED

	Number of Samples	Mean Error (ft/s)	Mean Error (knots)	Standard Deviation (ft/s)	Standard Deviation (knots)
Accelerometer complemented	1,202	1.4	0.8	7.1	4.2
Range limited with accelerometer complementation	1,202	8.0	4.7	6.3	3.7

KALMAN FILTER WITH VELOCITY OBSERVATIONS. The Kalman filter provided a method capable of extracting an optimum velocity estimate (in a mean-square sense) from the noisy observations of the DME. Figure 33 shows a block diagram of the implementation of the discrete time Kalman filter. The block labeled K(k) represents the updating of the Kalman gains based on the previous iteration as well as the updating of the covariance matrix based on the present data. The covariance matrix represents the mean-square error of the estimate. Therefore, the Kalman filter is a time-varying optimum statistical estimator which depends on the input and output to alter its filtering process.

Implementation of the Kalman filter required a model of the measurement process and a model for the dynamics of the process under measurement. The models were simple and incorporated statistics of the noisy DME range rate as well as some very simplified aircraft dynamics and maneuver statistics. A description of the development is contained in the appendix.

Figures 34 and 35 are plots of the output of the Kalman filter with a velocity input for the slowly varying groundspeed condition. Also plotted on these figures is INS groundspeed. Figure 34 represents the results obtained when using the Collins interrogator for this groundspeed condition, while figure 35 represents the results obtained with the King interrogator. A velocity limiter was used to prefilter the data prior to the Kalman filtering process. The velocity limiter range was from 125 ft/s to 325 ft/s (75 knots to 195 knots). The results of the filtering process for either interrogator are not satisfactory because of the lack of responsiveness in the case of the Collins interrogator, and the noisy output in the case of the King interrogator.

KALMAN FILTER WITH VELOCITY AND ACCELERATION OBSERVATIONS. The Kalman filter produces an optimum (mean-square) estimate of the state of a system. The filter depends on a measurement of the system's state, its own model of the dynamics of the system, and a description of the noise processes involved to provide such an estimate.

Performance of the filter is affected by the accuracy of the system model, the accuracy of the noise model, and the measurement made on the actual system. Generally, a more accurate system model will call for more states and the complexity (order) of the computations will increase. In the previous case, velocity was estimated based on noisy velocity samples and a system model (double integrator) whose state vector contains two entries, velocity and acceleration. By including acceleration in the measurement, the performance may be improved with a moderate increase in the computations required. The acceleration employed for this case was pitch-compensated longitudinal acceleration.

To eliminate the biases due to the acceleration term that were experienced in the accelerometer complementation algorithms, the acceleration term was high-passed to remove any bias errors prior to using it in the Kalman filter. A time-varying high-pass digital filter similar to the one developed for the accelerometer complementation scheme was used for this purpose. To compensate for attenuation of the lower frequency components, the filtered acceleration was multiplied by a gain factor greater than unity. The original filter equations (appendix) were revised to accommodate the newly included acceleration observation. This approach was utilized for both the Collins 860E-3 and the KDM-7000.

In the case of the KDM-7000, which provides no range rate filtering, the dynamic model is a suitable one. However, the Collins 860E-3 provides a 30-second low-pass range rate as the velocity observation. This would seemingly alter the signal dynamics and require a reformulation of the filter.

However, if the effect of the 30-second low-pass filter is modeled as an additive noise source, only the statistical noise descriptors will require modification. This was done, and the same filter equations were utilized for both the Collins 860E-3 and the King KDM-7000.

As done previously, the range rate input observations to the filter from the King DME were range limited to between 125 and 325 ft/s. This limiter was also used on the Collins DME range rate observations, but did not offer any improvement in the performance and therefore was not needed.

The filter was implemented in Fortran on a PDP 11/15. Raw data tapes recorded on previous test flights were filtered and plotted and statistics were computed using INS groundspeed as the reference.

Figures 36 through 41 are plots of the results using both velocity and acceleration as inputs to the filters. Figures 36 through 38 are the results when using the Collins DME in the three different groundspeed conditions, and figures 39 through 41 are the results when using the King DME. As can be seen, the addition of the acceleration observations to the Kalman filter greatly improve the tracking accuracy and responses of the measurement. Statistical summaries of the Kalman filter results for the Collins and the King interrogator are contained in tables 7 and 8.

TABLE 7. STATISTICAL ERROR SUMMARY OF RESULTS FOR KALMAN FILTERING ON COLLINS INTERROGATOR

	Number of Samples	Mean Error (ft/s)	Mean Error (knots)	Standard Deviation (ft/s)	Standard Deviation (knots)
STABLE GROUNDSPEED					
Velocity	1,547	0.4	0.2	6.0	3.5
Velocity and acceleration	1,547	0.2	0.1	5.9	3.5
SLOWLY VARYING GROUNDSPEED					
Velocity	1,500	5.0	3.4	8.5	5.0
Velocity and acceleration	1,500	-0.9	-0.5	7.0	4.1
RAPIDLY VARYING GROUNDSPEED					
Velocity	1,499	2.8	1.7	12.7	7.5
Velocity and acceleration	1,499	0.6	0.4	6.1	3.6

TABLE 8. STATISTICAL ERROR SUMMARY OF RESULTS FOR KALMAN FILTERING ON KING INTERROGATOR

	Number of Samples	Mean Error (ft/s)	Mean Error (knots)	Standard Deviation (ft/s)	Standard Deviation (knots)
STABLE GROUNDSPEED					
Velocity	1,479	2.3	1.4	13.6	8.0
Velocity and acceleration	1,479	-2.6	-1.5	2.8	1.6
SLOWLY VARYING GROUNDSPEED					
Velocity	1,222	-1.4	-0.8	10.4	6.1
Velocity and acceleration	1,222	6.5	3.8	4.5	2.7
RAPIDLY VARYING GROUNDSPEED					
Velocity	1,202	-5.4	-3.2	14.6	8.6
Velocity and acceleration	1,202	-5.9	-3.5	6.1	3.6

CONCLUSION

Based on the tests conducted, it is concluded that responsive and accurate groundspeed can be obtained from an ARINC characteristic 568 DME. By utilizing suitable interface circuitry to make use of the range rate pulse output and suitable digital filtering, groundspeed outputs with a standard deviation of about 3 knots when compared to INS groundspeed were typically obtained. Response of the digital filter was such that there was no time lag between the groundspeed output of the filter and the groundspeed output of the INS. The techniques utilized lend themselves to microprocessor technology for hardware implementation and require no modification to either the airborne or ground DME equipment.

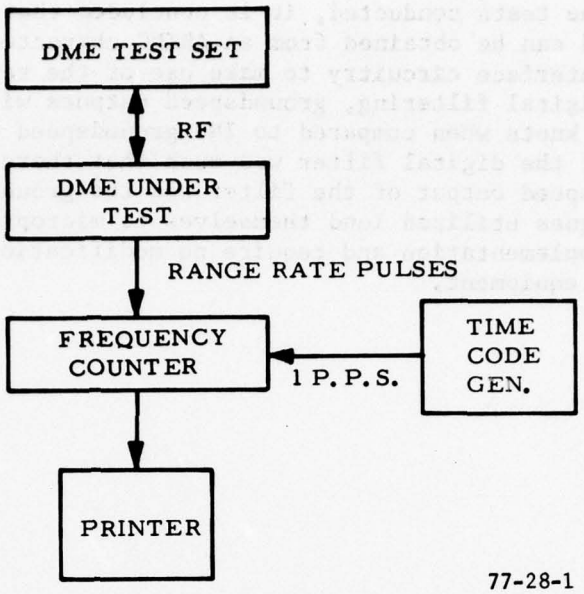

FIGURE 1. DME LABORATORY TEST SETUP

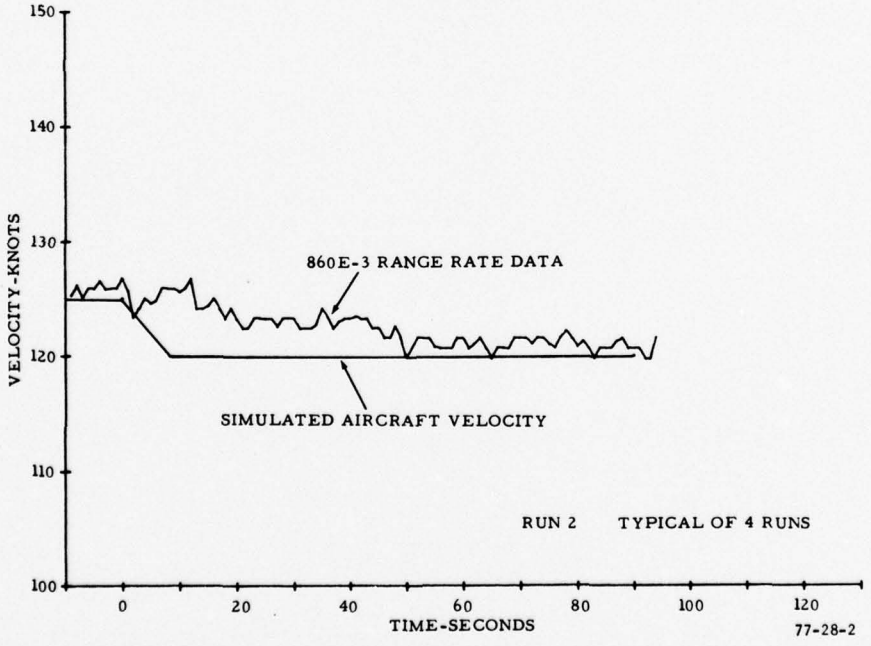

FIGURE 2. COLLINS 860E-3 INTERROGATOR RANGE RATE RESPONSE FOR VELOCITY CHANGE OF -5 KNOTS

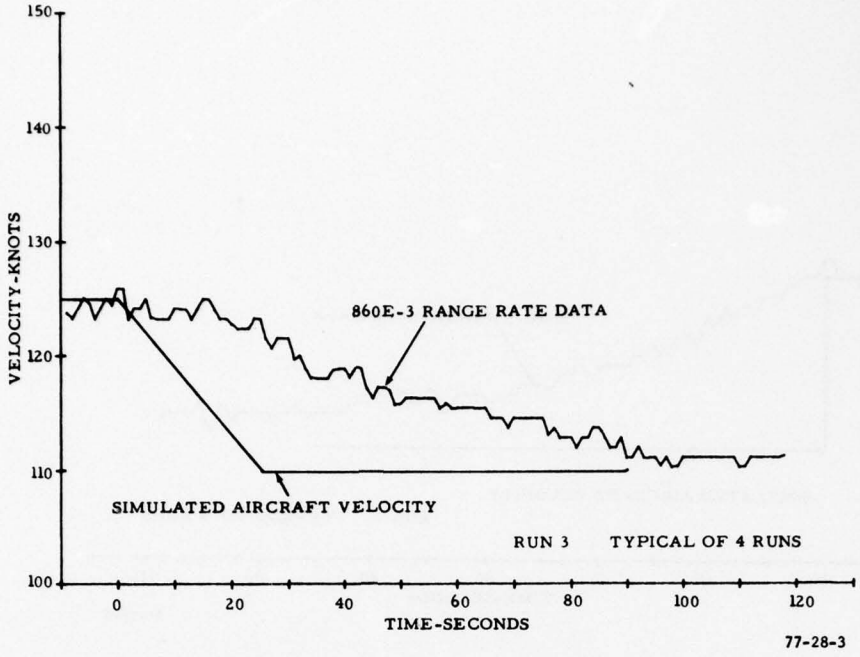

FIGURE 3. COLLINS 860E-3 INTERROGATOR RANGE RATE RESPONSE FOR VELOCITY CHANGE OF -15 KNOTS

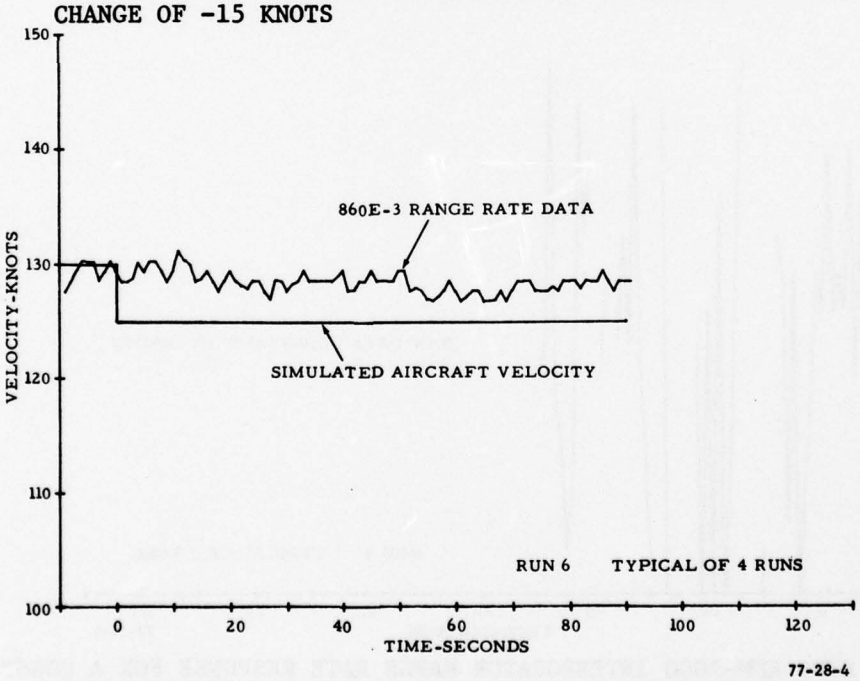

FIGURE 4. COLLINS 860E-3 INTERROGATOR RANGE RATE RESPONSE FOR A STEP VELOCITY CHANGE OF -5 KNOTS

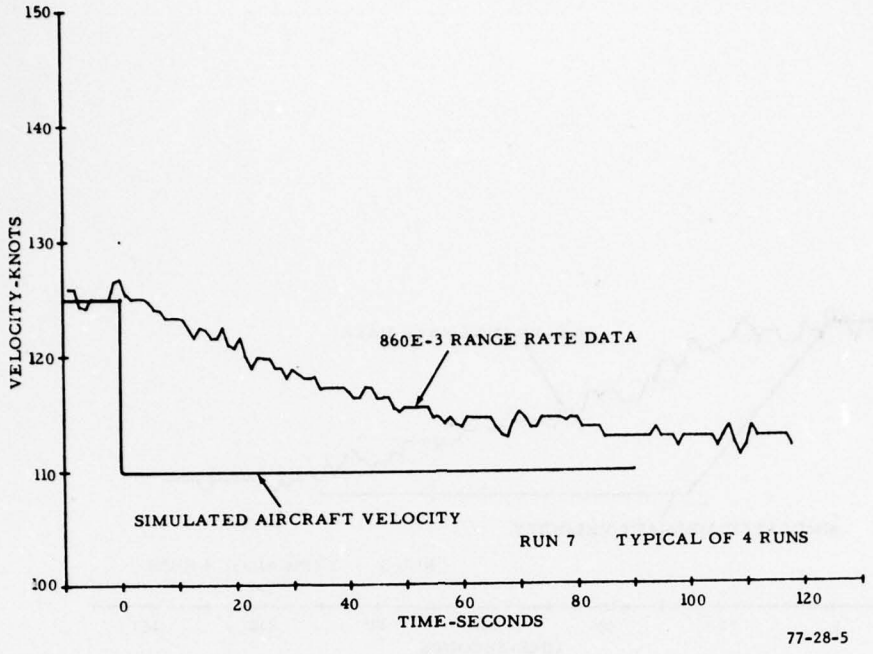

FIGURE 5. COLLINS 860E-3 INTERROGATOR RANGE RATE RESPONSE FOR A STEP VELOCITY CHANGE OF -15 KNOTS

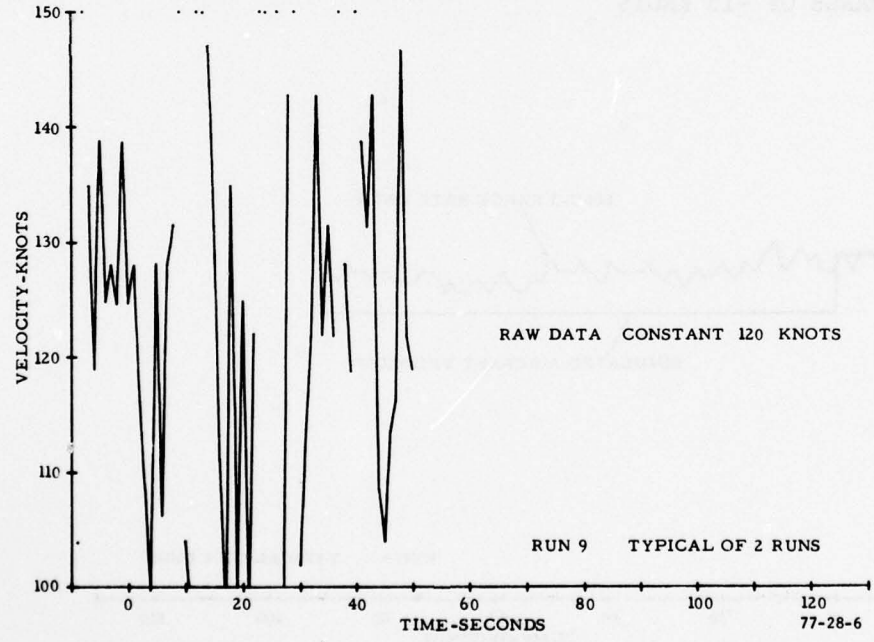

FIGURE 6. KING KDM-7000 INTERROGATOR RANGE RATE RESPONSE FOR A CONSTANT VELOCITY OF 120 KNOTS

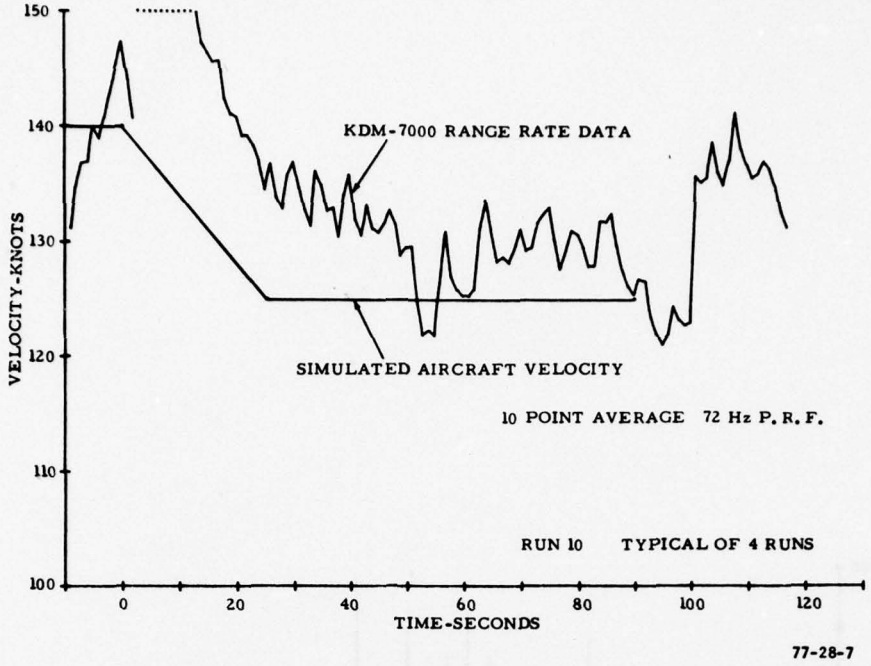

FIGURE 7. KING KDM-7000 INTERROGATOR RANGE RATE RESPONSE FOR A VELOCITY CHANGE OF -15 KNOTS

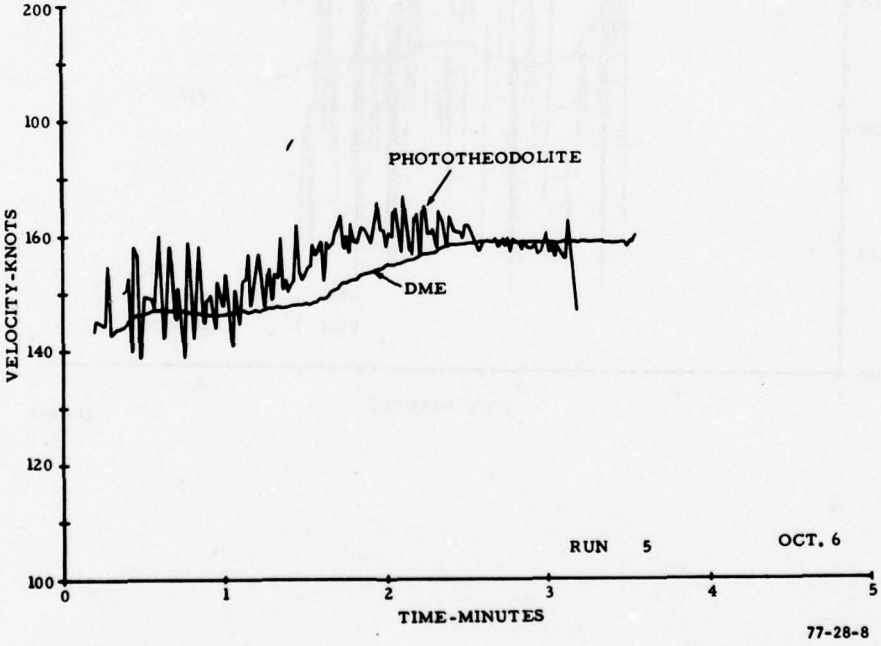

FIGURE 8. COLLINS 860E-3 INTERROGATOR RANGE RATE RESPONSE FOR AN AIRBORNE ACCELERATION RUN

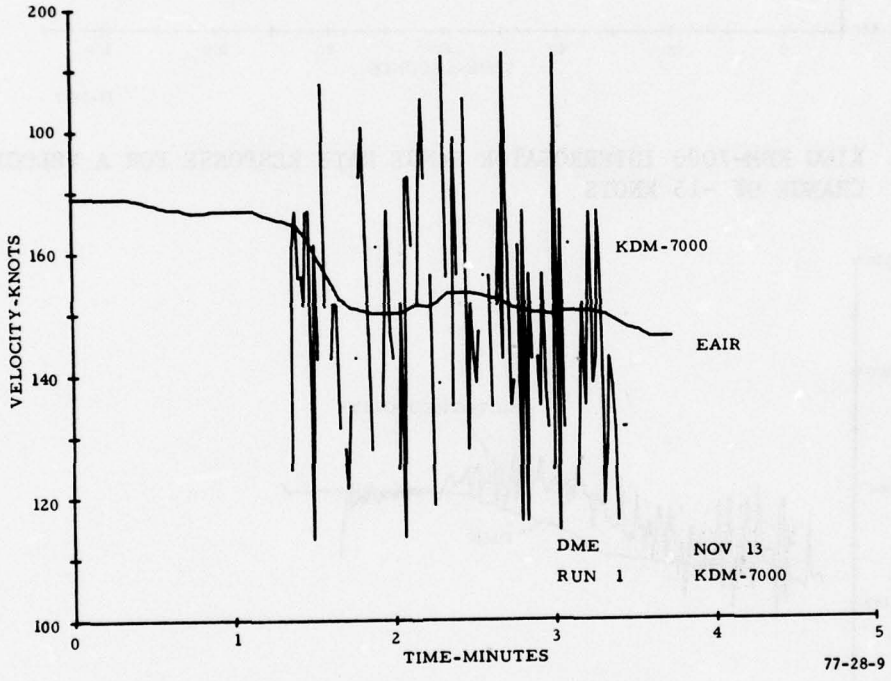

FIGURE 9. KING KDM-7000 INTERROGATOR RANGE RATE RESPONSE FOR AN AIRBORNE DECELERATION RUN

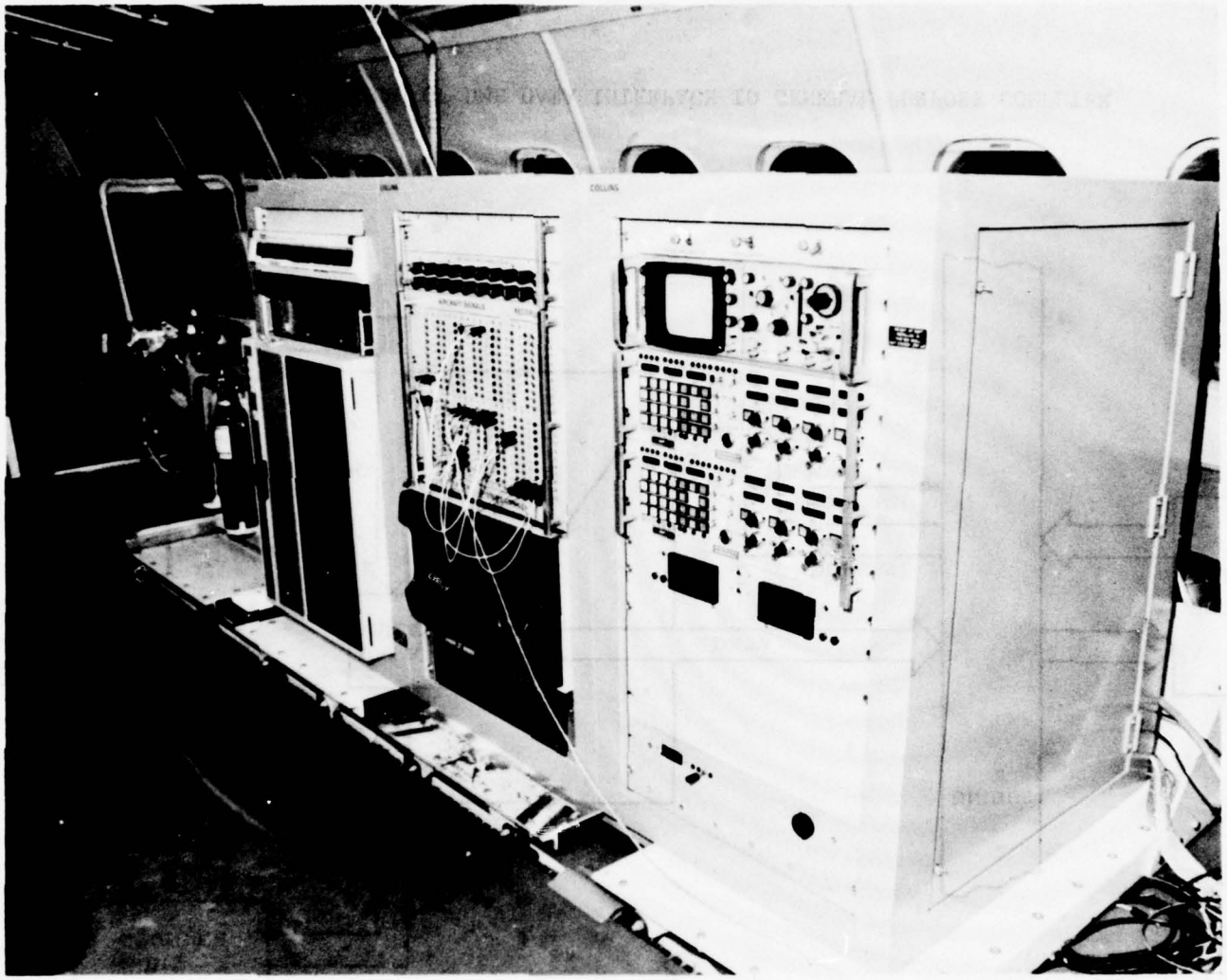

77-28-10

FIGURE 10. GENERAL PUTPOSE DIGITAL COMPUTER INSTALLATION IN TEST BED AIRCRAFT N-42, A CV880

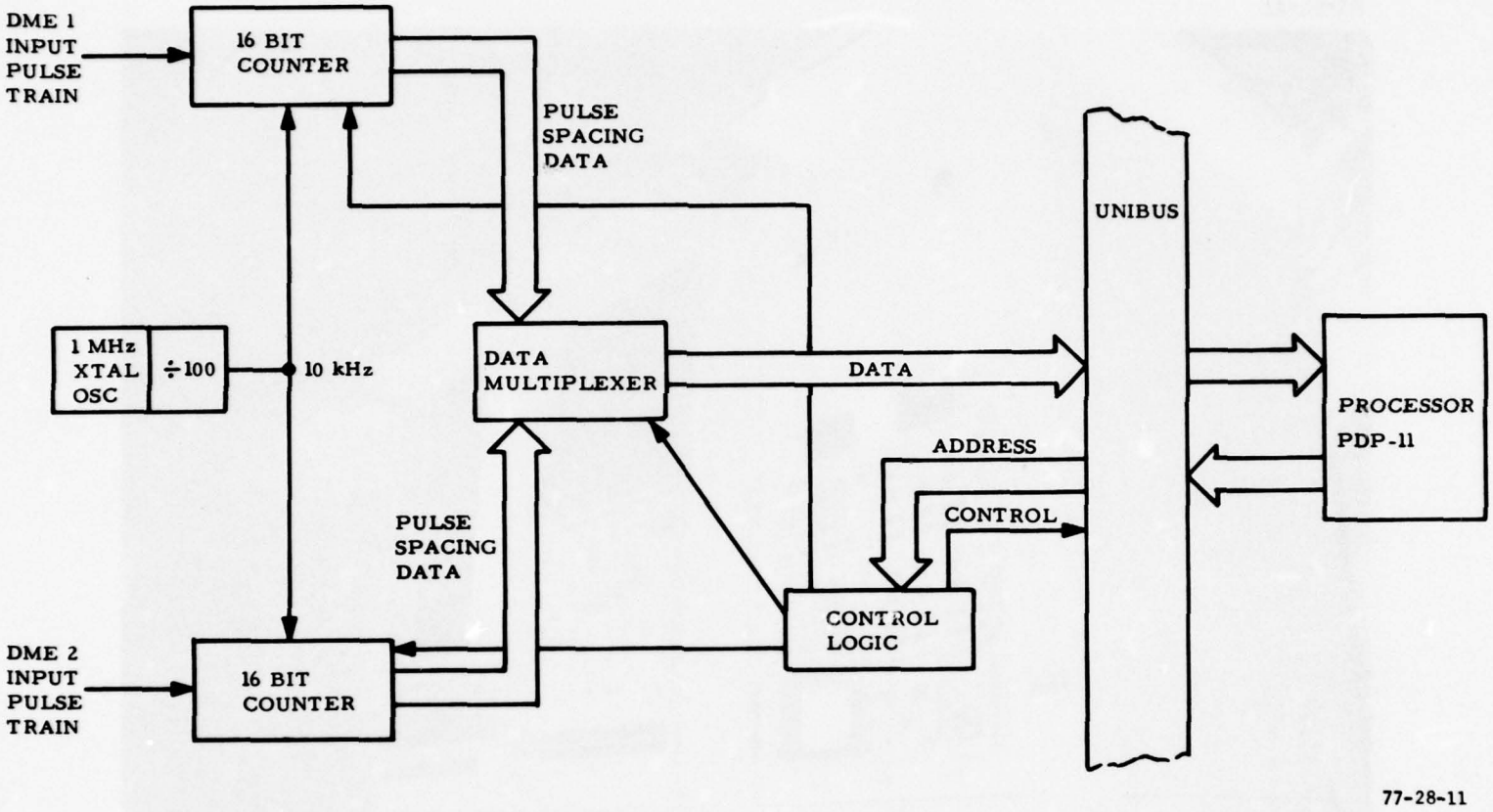

FIGURE 11. BLOCK DIAGRAM OF DME DATA INTERFACE TO GENERAL PURPOSE COMPUTER

LEAD LAG COMPENSATION

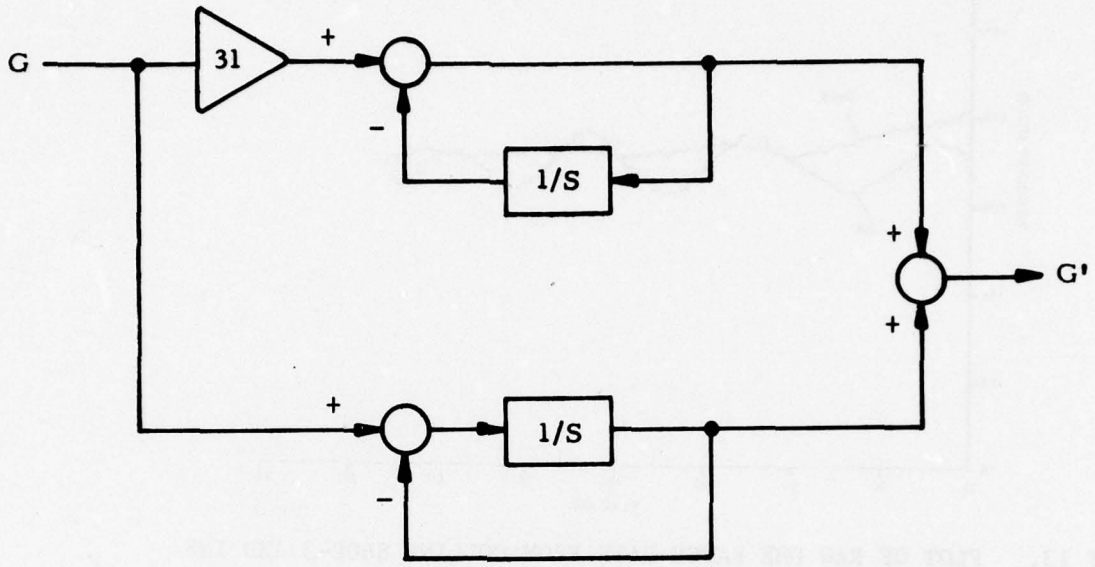

$$G' = \left(\frac{31S + 1}{S + 1}\right) G$$

$$G = \left(\frac{1}{30S + 1}\right) G_{ideal}$$

$$G' = \left(\frac{1}{30S + 1}\right)\left(\frac{31S + 1}{S + 1}\right) G_{ideal}$$

$$G' \approx G_{ideal}$$

G = 30 SECOND LAGGED DME RANGE RATE
G'= COMPENSATED DME RANGE RATE
G_{ideal} = ideal (TRUE) RANGE RATE

77-28-12

FIGURE 12. BLOCK DIAGRAM OF LEAD/LAG COMPENSATION

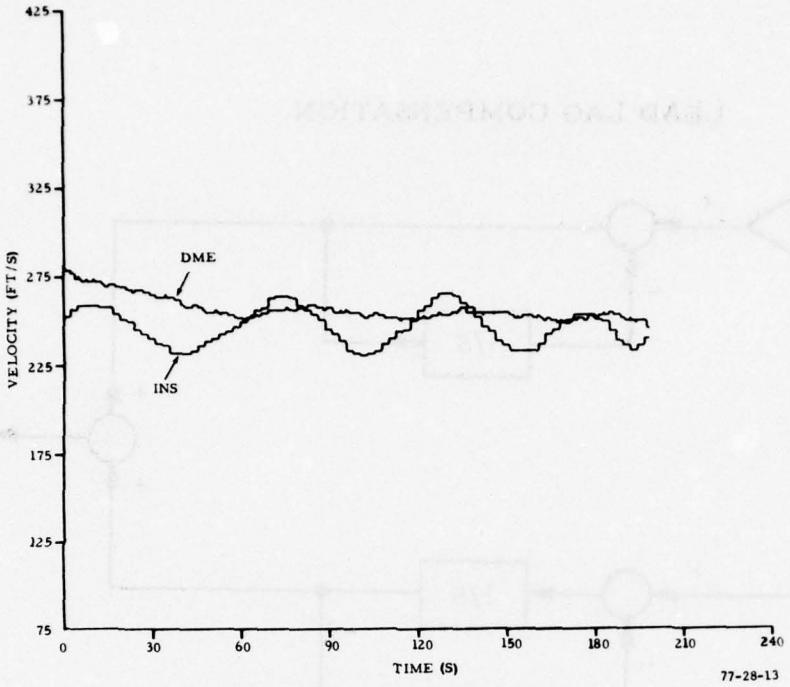

FIGURE 13. PLOT OF RAW DME RANGE RATE FROM COLLINS 860E-3 AND INS GROUNDSPEED FOR A TEST APPROACH

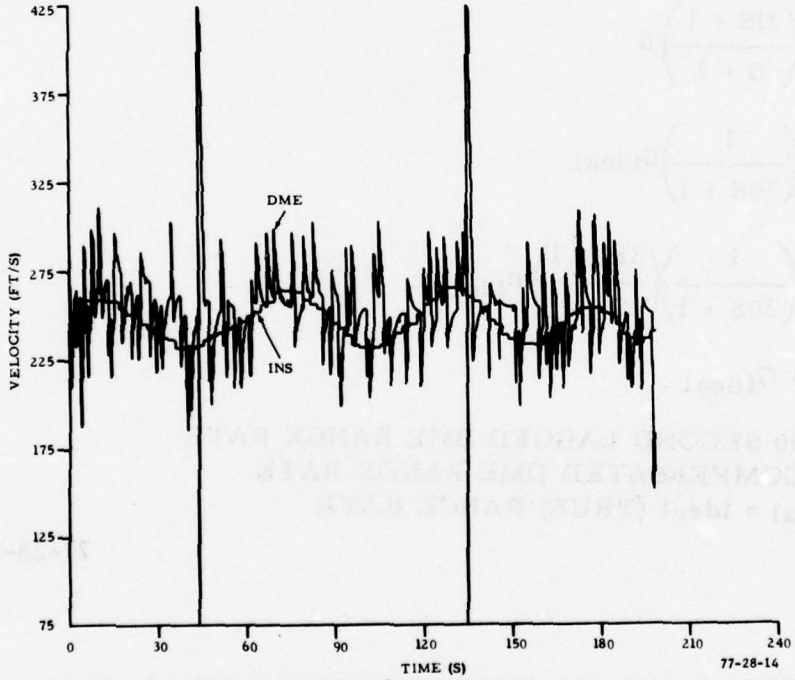

FIGURE 14. PLOT OF OUTPUT OF LEAD/LAG FILTER AND INS GROUNDSPEED FOR A TEST APPROACH

RAW RANGE RATE (fps)	LEAD/LAG. OUTPUT (fps)	
215.7521	215.7521	
215.7521	215.7521	
→ 215.7521	215.7522	
→ 216.9223	250.3577	
216.9223	247.1732	
216.9223	244.2921	
216.2136	220.7269	
216.2136	220.2966	
→ 216.2136	219.9073	
→ 215.3730	194.6976	
215.3730	196.6667	
→ 215.3730	198.4483	
→ 214.4664	173.2530	
214.4664	177.1780	
→ 214.4664	180.7292	
→ 213.9390	168.3455	
213.9390	172.6876	
212.7358	141.0361	
212.7358	147.8648	
212.7358	154.0432	
212.4391	150.8597	
212.4391	156.7241	
212.4391	162.0299	
212.4391	166.8304	
212.4391	171.1737	
212.4391	175.1034	
212.5215	181.0954	
212.5215	184.0879	
212.5215	186.7955	
212.4391	186.8087	
212.4391	189.2493	→= RAW RANGE RATE CHANGES
212.4391	191.4575	
212.4391	193.4554	
212.4391	195.2630	
→ 212.4391	196.8985	
→ 213.6423	233.9587	
213.6423	232.0236	

77-28-15

FIGURE 15. PRINTOUT OF INPUT TO AND OUTPUT FROM LEAD/LAG FILTER

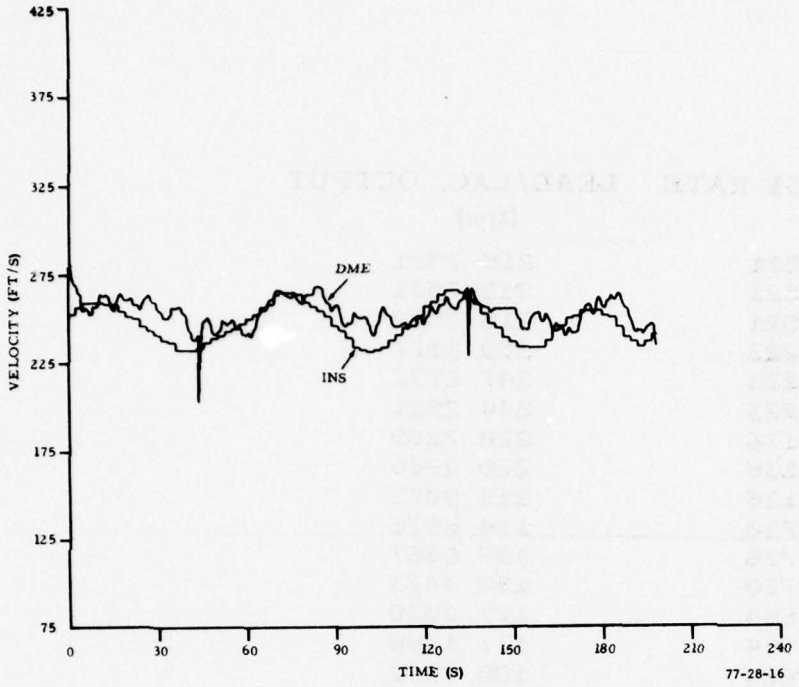

FIGURE 16. PLOT OF OUTPUT OF LEAD/LAG FILTER AND INS GROUNDSPEED WITH A 5-SECOND LOW-PASS FILTER ON INPUT TO LEAD/LAG FILTER

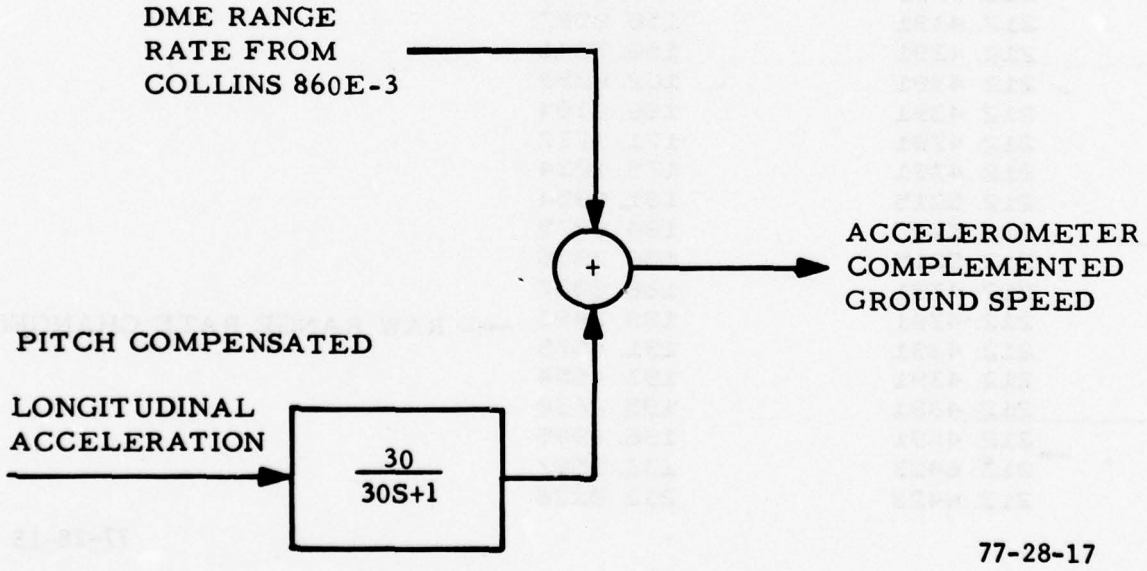

FIGURE 17. BLOCK DIAGRAM OF ACCELEROMETER COMPLEMENTATION FOR COLLINS 860E-3 INTERROGATOR

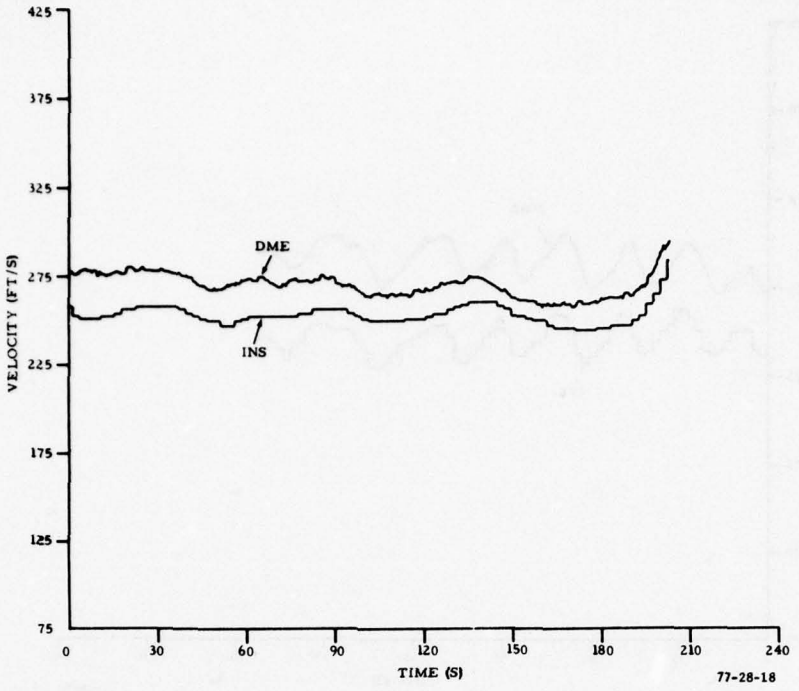

FIGURE 18. PLOT OF COLLINS 860E-3 ACELEROMETER-COMPLEMENTED RANGE RATE FOR A STABLE GROUNDSPEED TEST APPRAOCH

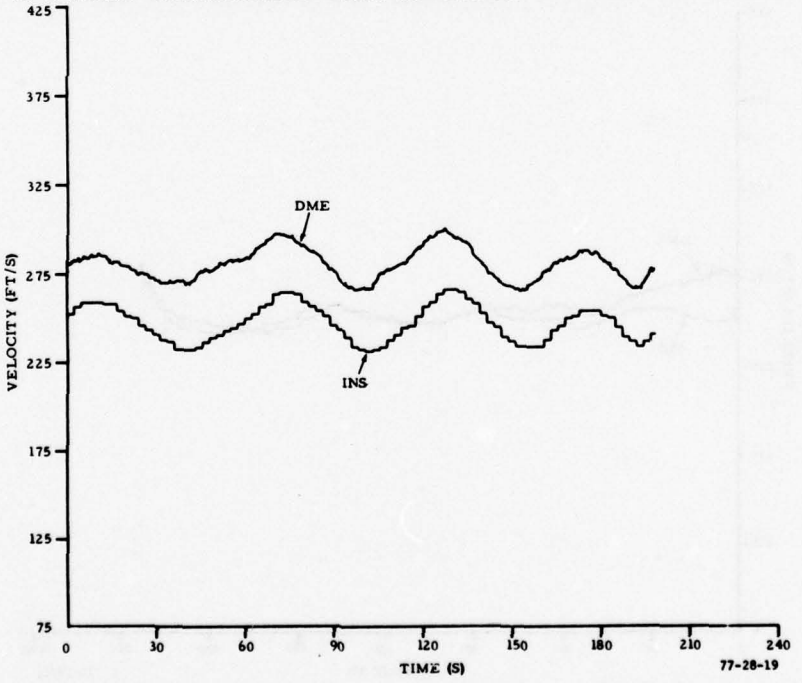

FIGURE 19. PLOT OF COLLINS 860E-3 ACCELEROMETER-COMPLEMENTED RANGE RATE FOR A SLOWLY VARYING GROUNDSPEED TEST APPROACH

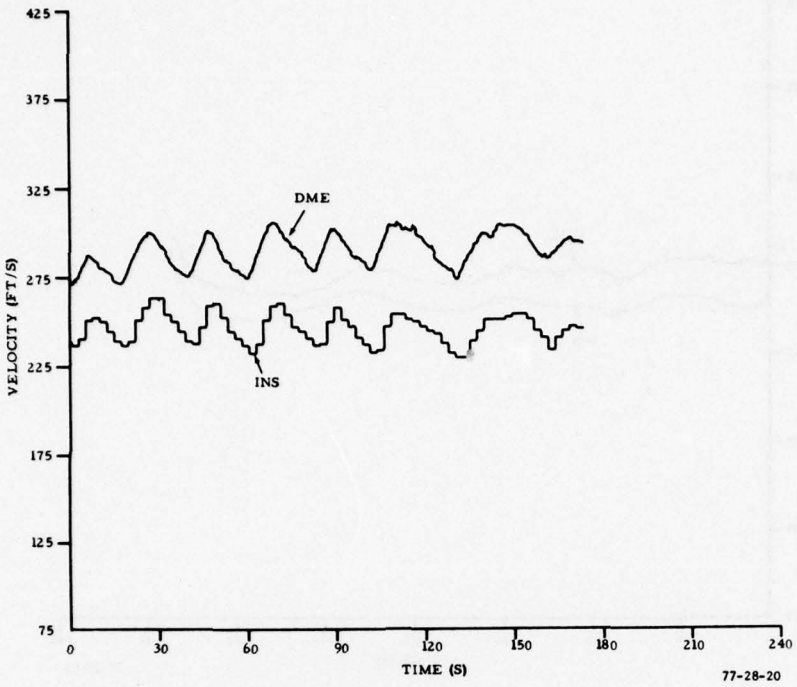

FIGURE 20. PLOT OF COLLINS 860E-3 ACCELEROMETER-COMPLEMENTED RANGE RATE FOR A RAPIDLY VARYING GROUNDSPEED TEST APPROACH

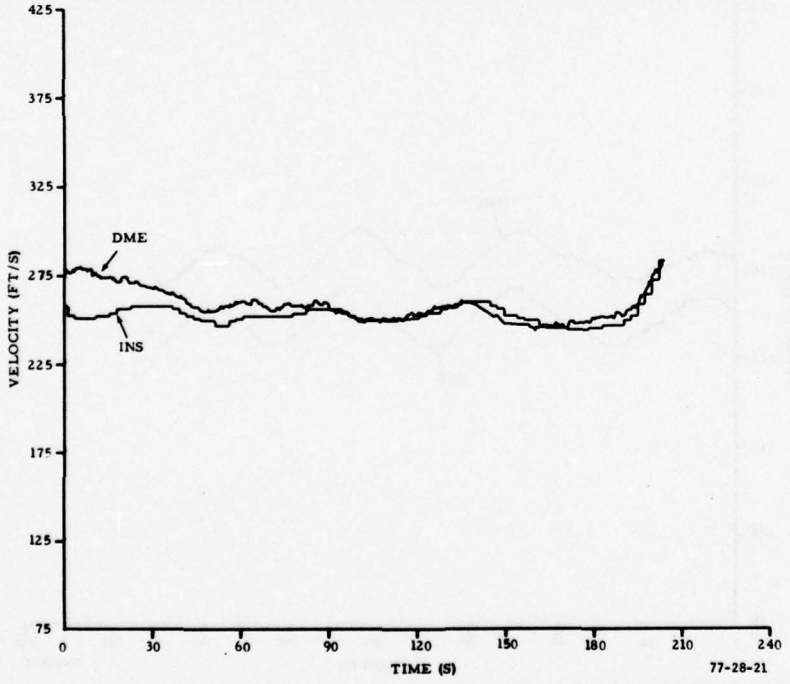

FIGURE 21. PLOT OF COLLINS 860E-3 TIME-VARYING ACCELEROMETER-COMPLEMENTED RANGE RATE FOR A STABLE GROUNDSPEED TEST APPROACH

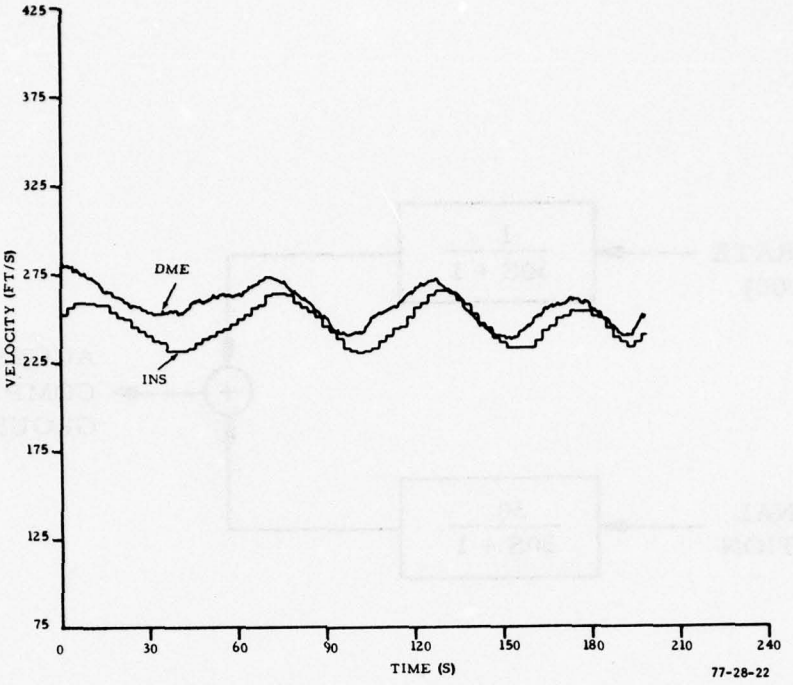

FIGURE 22. PLOT OF COLLINS 860E-3 TIME-VARYING ACCELEROMETER-COMPLEMENTED RANGE RATE FOR A SLOWLY VARYING GROUNDSPEED TEST APPROACH

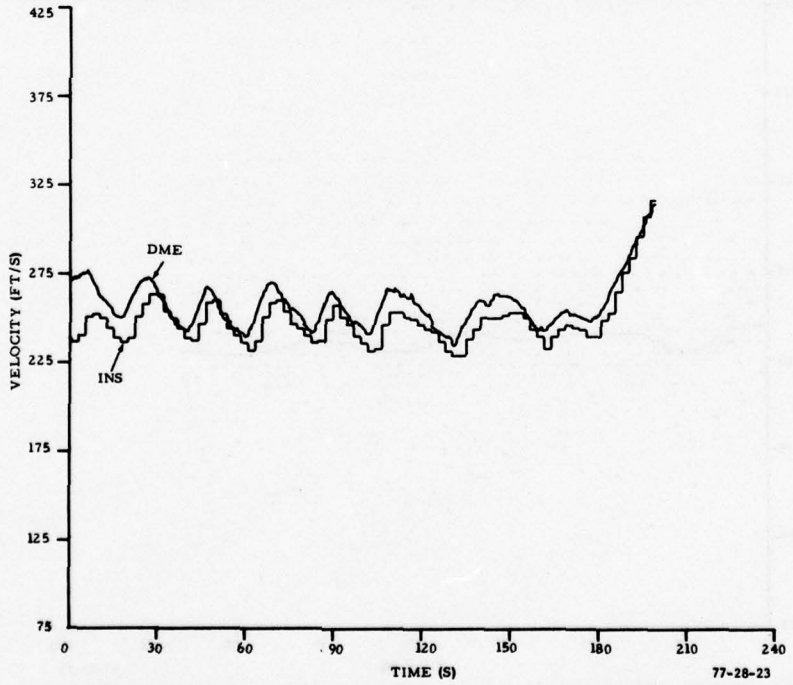

FIGURE 23. PLOT OF COLLINS 860E-3 TIME-VARYING ACCELEROMETER-COMPLEMENTED RANGE RATE FOR A RAPIDLY VARYING GROUNDSPEED TEST APPROACH

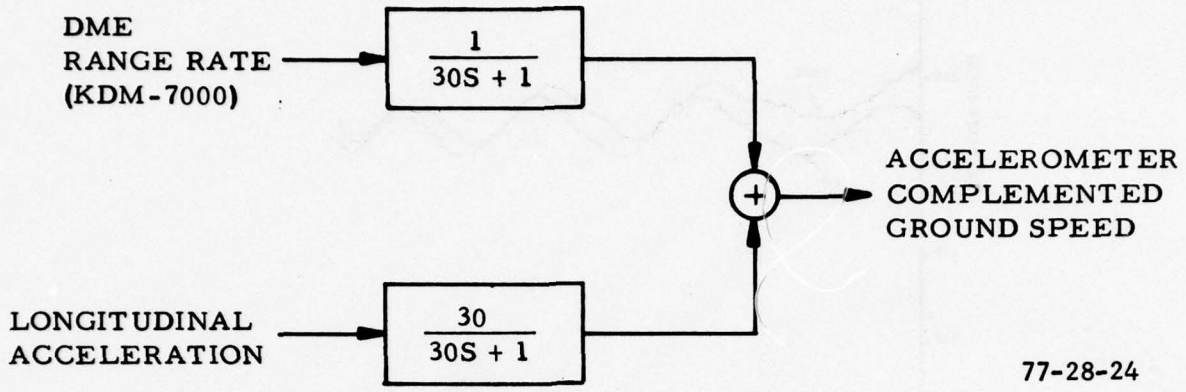

FIGURE 24. BLOCK DIAGRAM OF ACCELEROMETER COMPLEMENTATION FOR KING KDM-7000

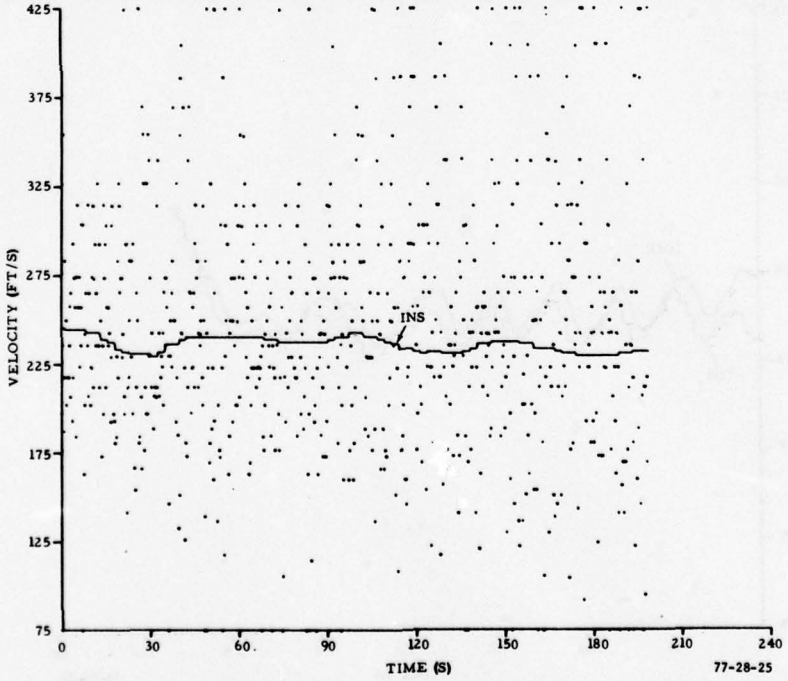

FIGURE 25. PLOT OF RAW DME RANGE RATE FROM KING KDM-7000 AND INS GROUNDSPEED FOR A TEST APPROACH

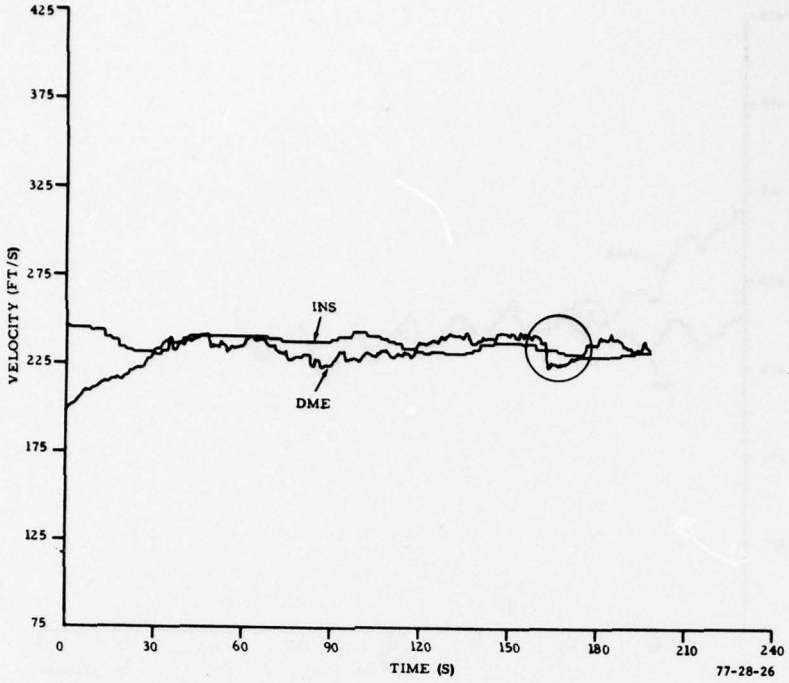

FIGURE 26. PLOT OF KING KDM-7000 TIME-VARYING ACCELEROMETER-COMPLEMENTED RANGE RATE FOR A STABLE GROUNDSPEED TEST APPROACH

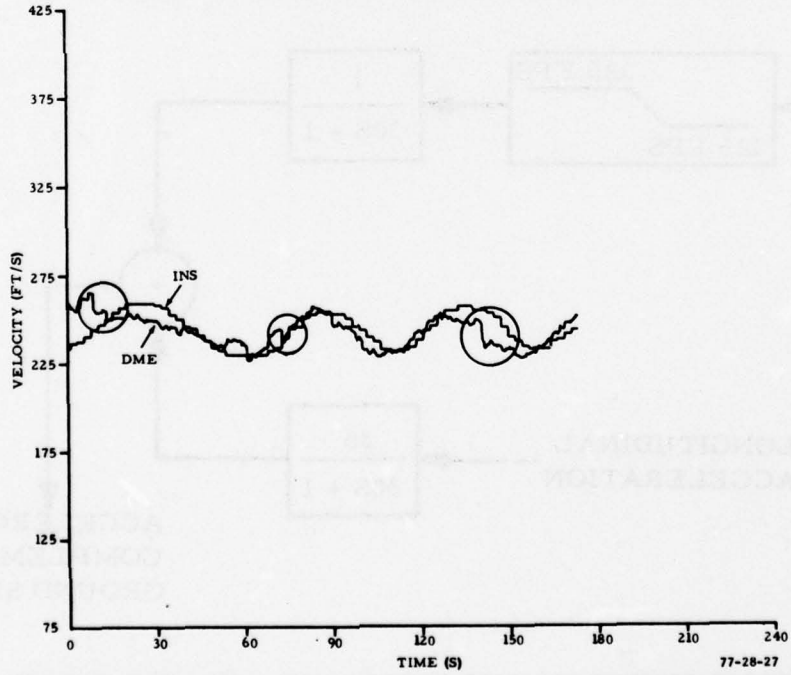

FIGURE 27. PLOT OF KING KDM-7000 TIME-VARYING ACCELEROMETER-COMPLEMENTED RANGE RATE FOR A SLOWLY VARYING GROUNDSPEED TEST APPROACH

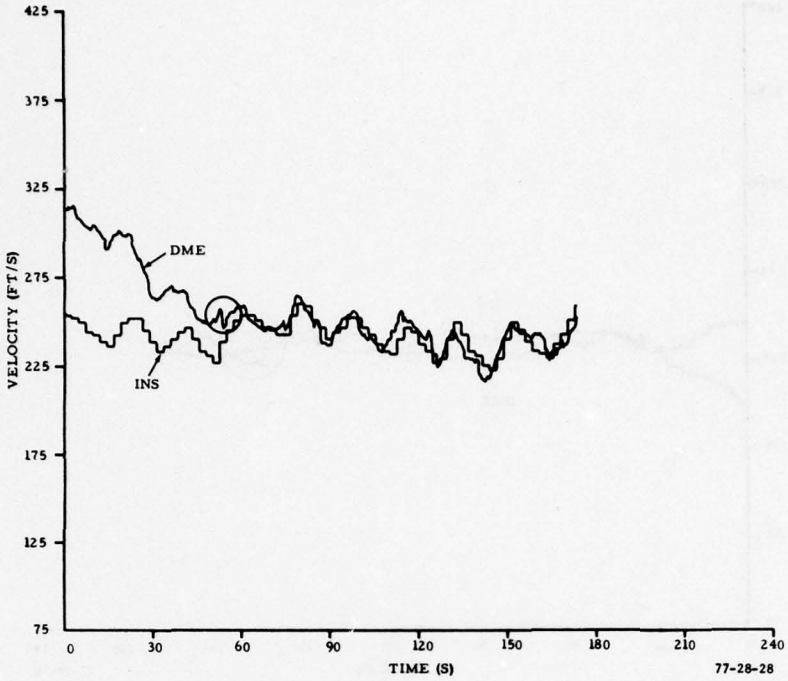

FIGURE 28. PLOT OF KING KDM-7000 TIME-VARYING ACCELEROMETER-COMPLEMENTED RANGE RATE FOR A RAPIDLY VARYING GROUNDSPEED TEST APPROACH

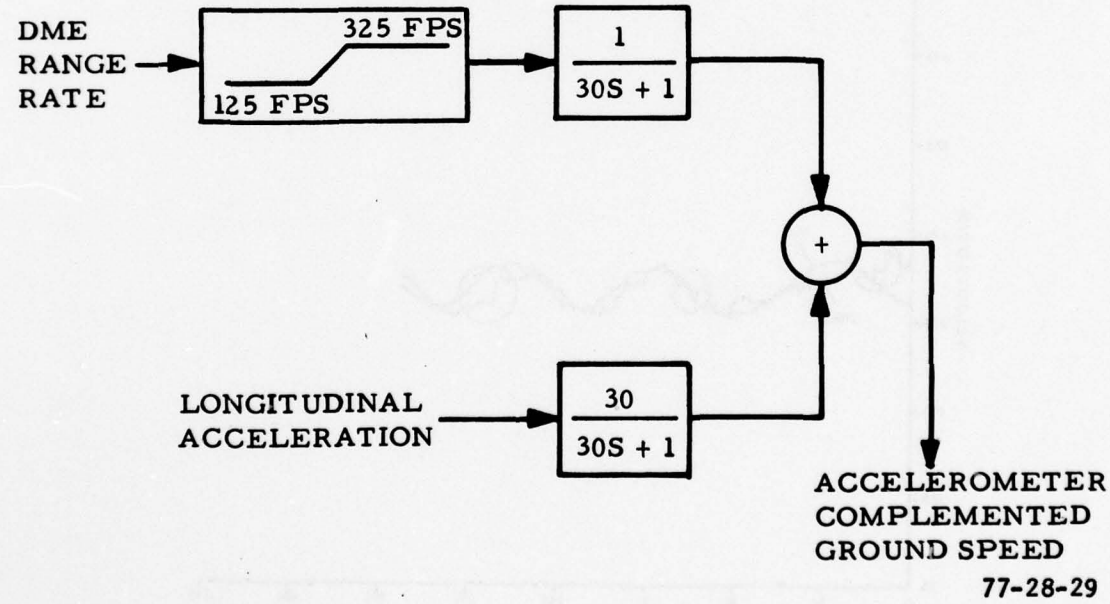

FIGURE 29. BLOCK DIAGRAM OF RANGE RATE LIMITING AND ACCELEROMETER COMPLEMENTATION FOR KING KDM-7000

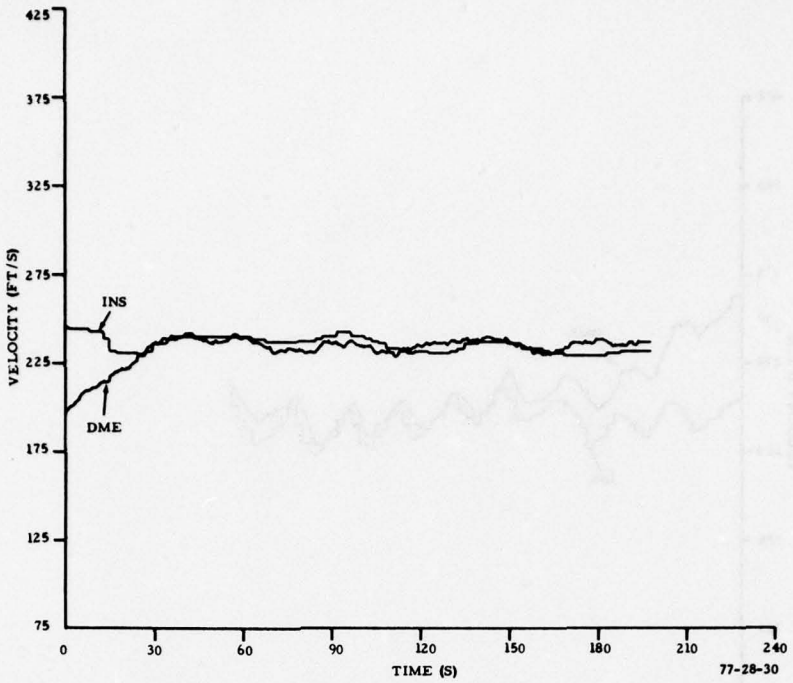

FIGURE 30. PLOT OF KING KDM-7000 NONLINEAR TIME-VARYING ACCELEROMETER-COMPLEMENTED RANGE RATE FOR A STABLE GROUNDSPEED TEST APPROACH

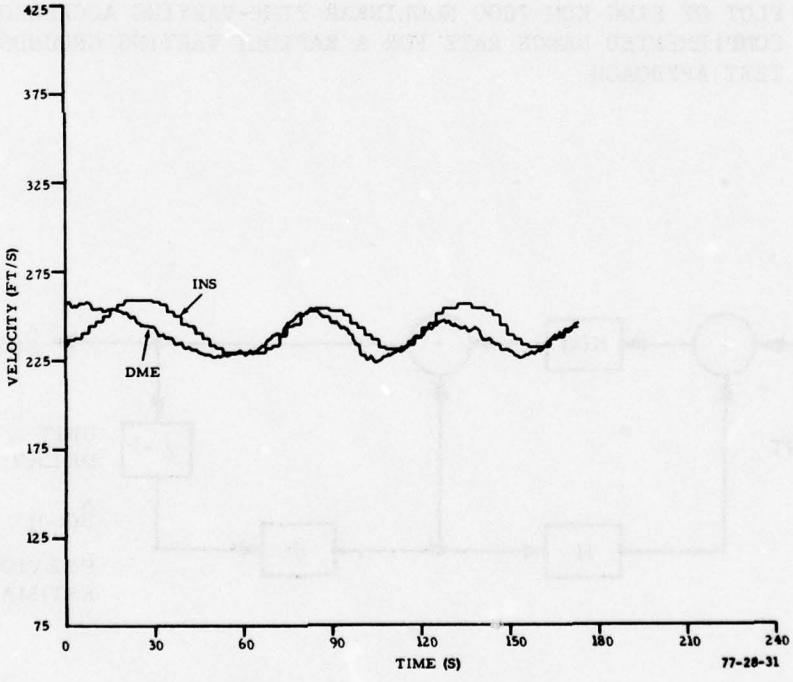

FIGURE 31. PLOT OF KING KDM-7000 NONLINEAR TIME-VARYING ACCELEROMETER-COMPLEMENTED RANGE RATE FOR A SLOWLY VARYING GROUNDSPEED TEST APPROACH

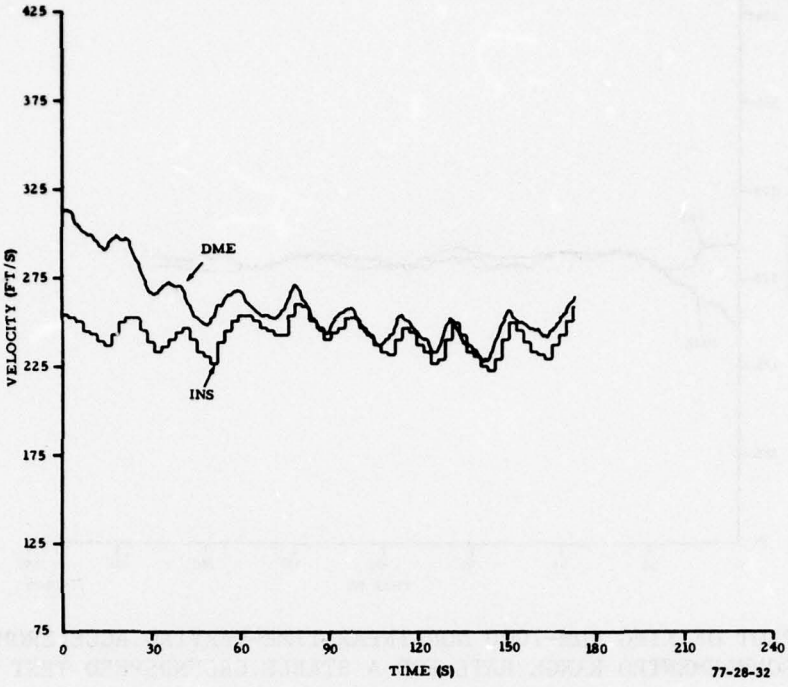

FIGURE 32. PLOT OF KING KDM-7000 NONLINEAR TIME-VARYING ACCELEROMETER-COMPLEMENTED RANGE RATE FOR A RAPIDLY VARYING GROUNDSPEED TEST APPROACH

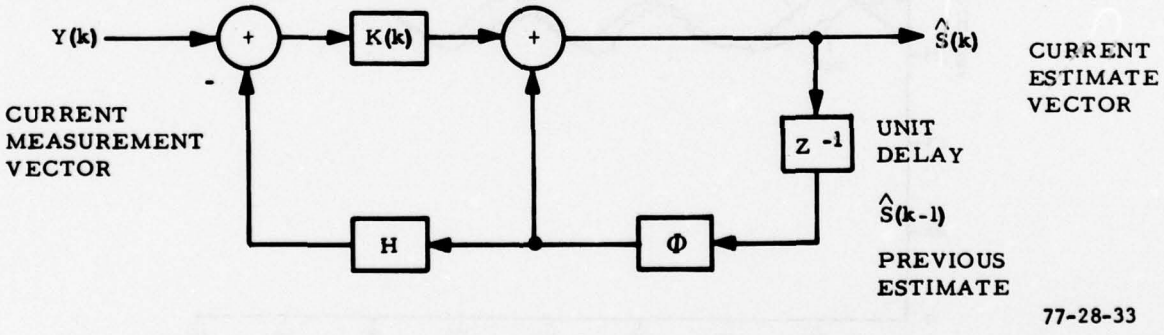

FIGURE 33. BLOCK DIAGRAM OF IMPLEMENTATION OF KALMAN FILTER

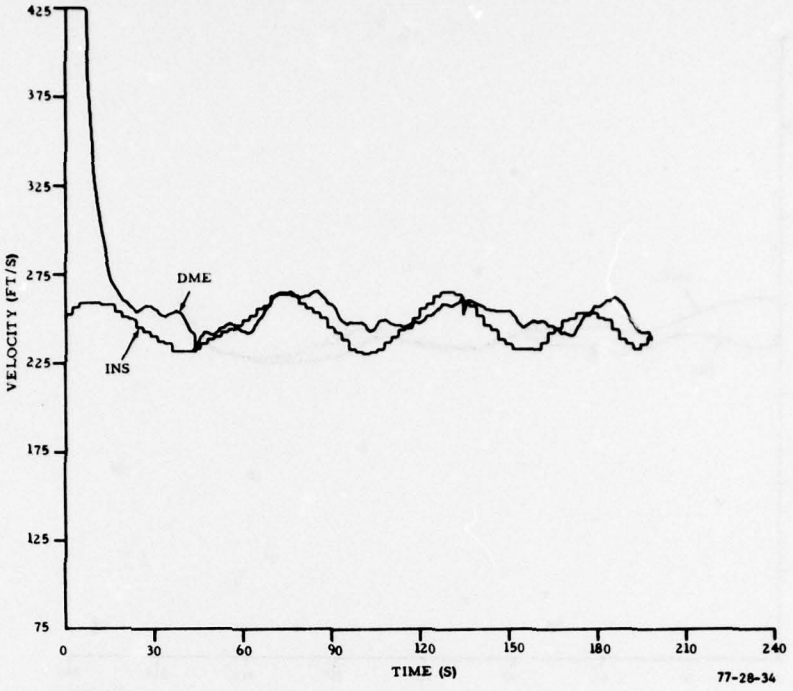

FIGURE 34. PLOT OF COLLINS 860E-3 RANGE RATE WITH KALMAN FILTERING (VELOCITY OBSERVATIONS) AND INS GROUNDSPEED FOR A TEST APPROACH

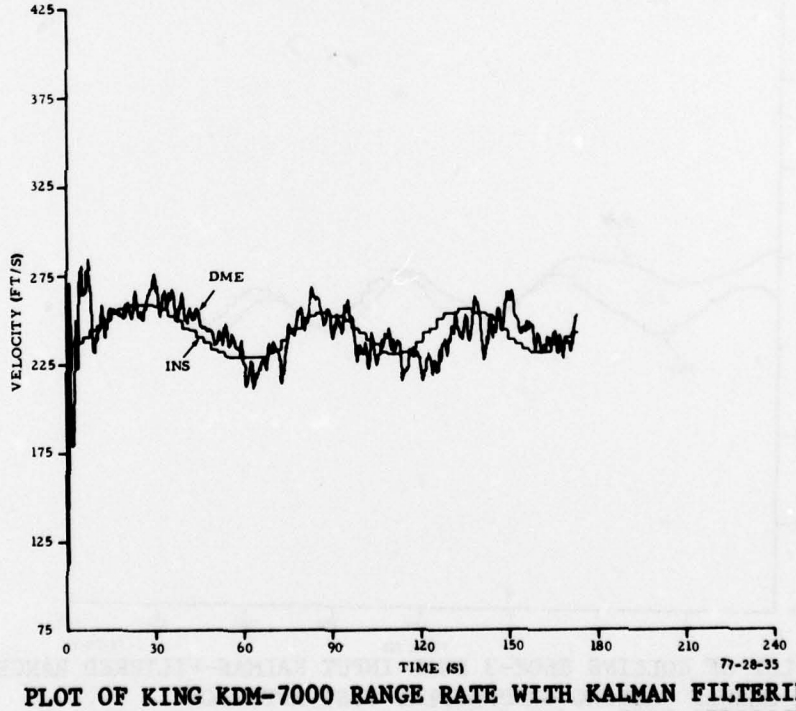

FIGURE 35. PLOT OF KING KDM-7000 RANGE RATE WITH KALMAN FILTERING (VELOCITY OBSERVATIONS) AND INS GROUNDSPEED FOR A TEST APPROACH

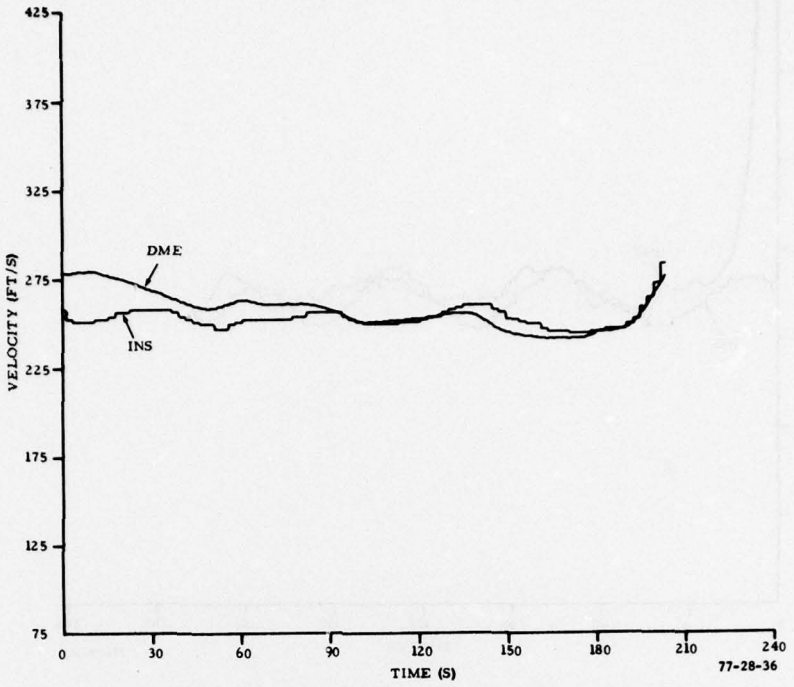

FIGURE 36. PLOT OF COLLINS 860E-3 DUAL-INPUT KALMAN-FILTERED RANGE RATE FOR A STABLE GROUNDSPEED TEST APPROACH

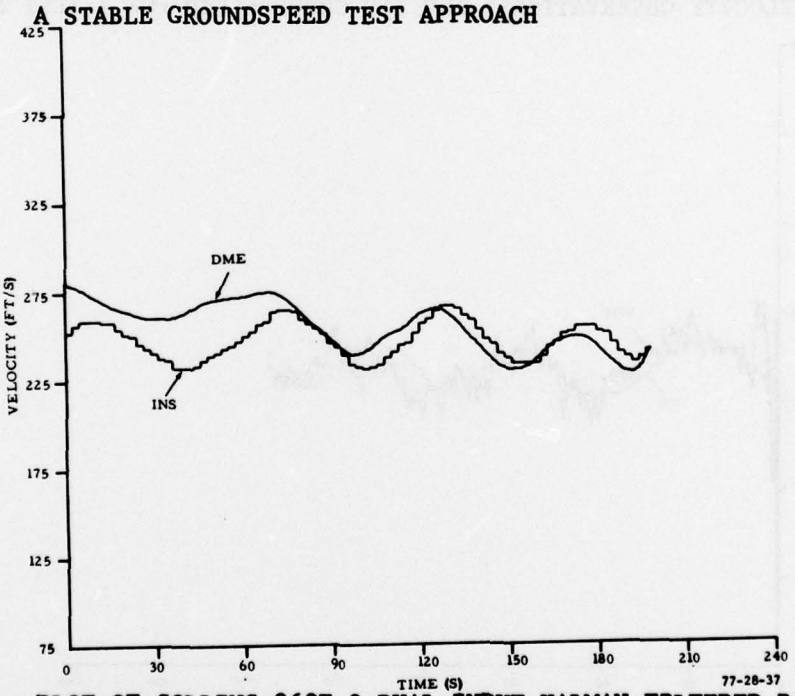

FIGURE 37. PLOT OF COLLINS 860E-3 DUAL-INPUT KALMAN-FILTERED RANGE RATE FOR A SLOWLY VARYING GROUNDSPEED TEST APPROACH

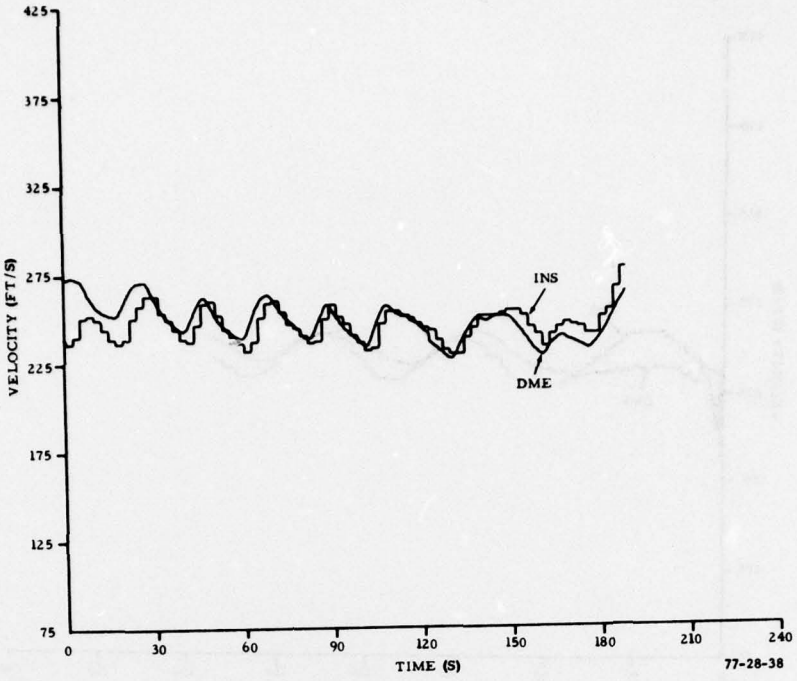

FIGURE 38. PLOT OF COLLINS 860E-3 DUAL-INPUT KALMAN-FILTERED RANGE RATE FOR A RAPIDLY VARYING GROUNDSPEED TEST APPROACH

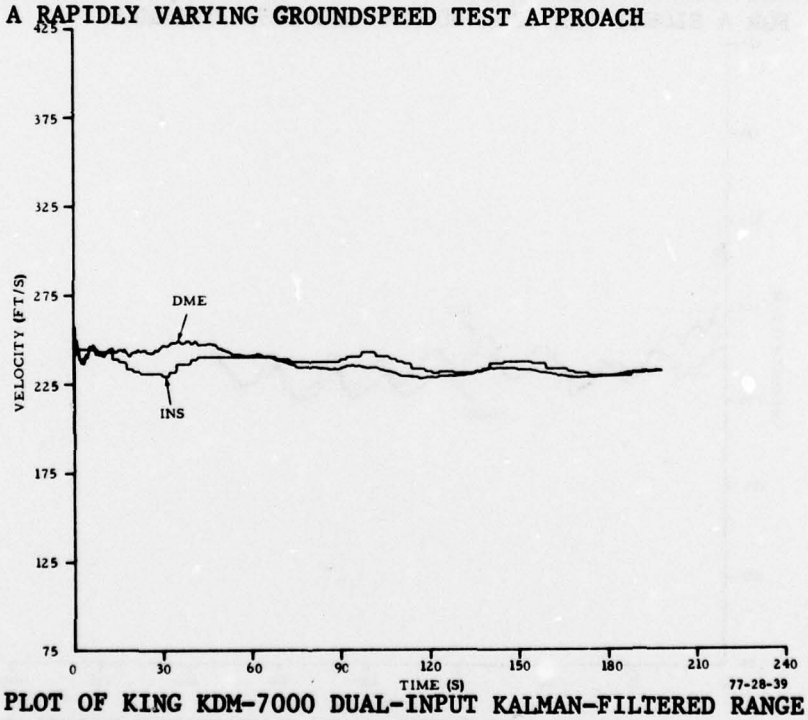

FIGURE 39. PLOT OF KING KDM-7000 DUAL-INPUT KALMAN-FILTERED RANGE RATE FOR A STABLE GROUNDSPEED TEST APPROACH

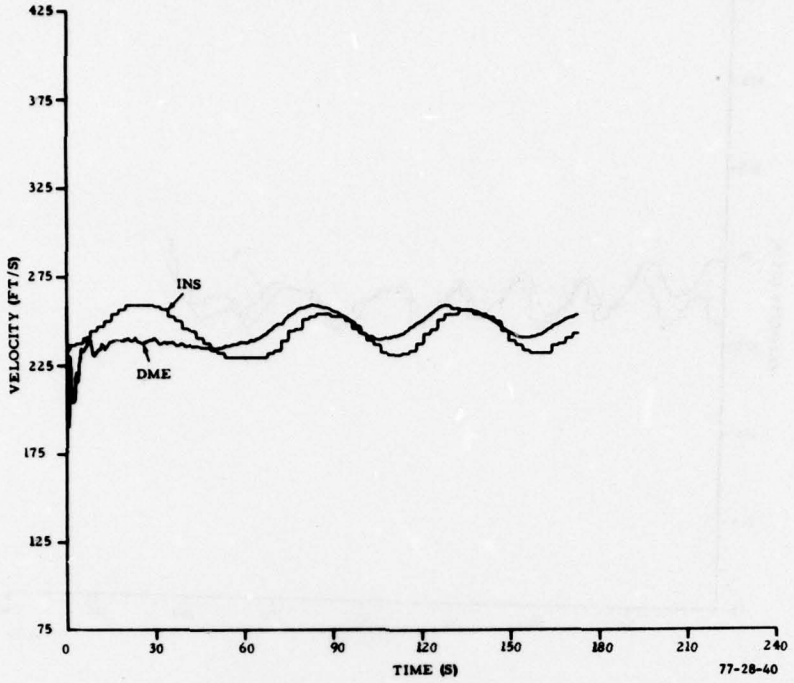

FIGURE 40. PLOT OF KING KDM-7000 DUAL-INPUT KALMAN-FILTERED RANGE RATE FOR A SLOWLY VARYING GROUNDSPEED TEST APPROACH

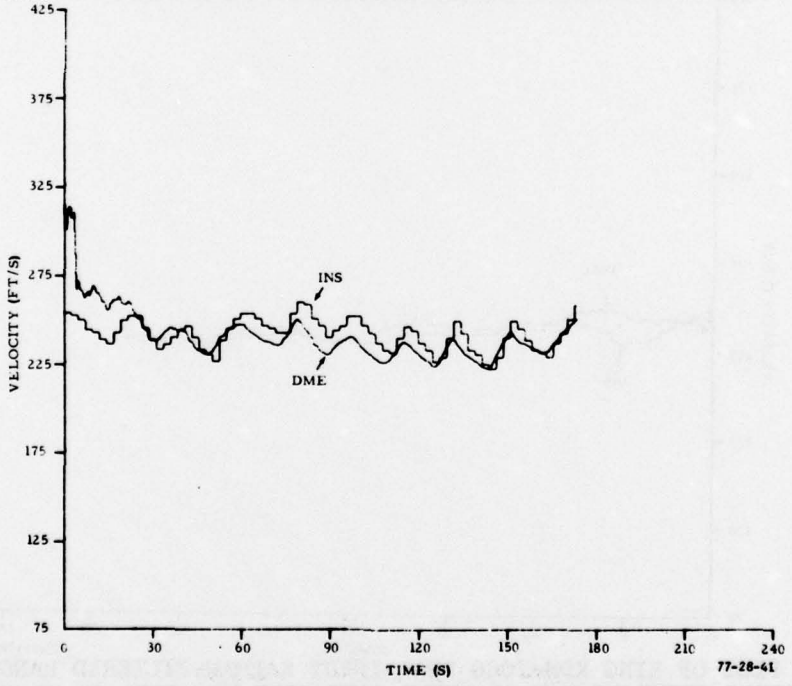

FIGURE 41. PLOT OF KING KDM-7000 DUAL-INPUT KALMAN-FILTERED RANGE RATE FOR A RAPIDLY VARYING GROUNDSPEED TEST APPROACH

APPENDIX A

STATISTICAL ESTIMATOR DESIGN FOR DME-DERIVED GROUNDSPEED

LIST OF ILLUSTRATIONS

STATISTICAL ESTIMATOR DESIGN FOR DME-DERIVED GROUNDSPEED

KALMAN FILTER TECHNIQUE.

The range rate output of the King DME is an extremely noisy signal. It is possible, however, to estimate the state (velocity) of the dynamic system (aircraft) from observations contaminated by noise. The problem may be approached by utilizing theory and techniques for designing statistical state estimators (Kalman filter).

The Kalman filter provided a method capable of extracting an optimum velocity estimate (in a mean-square sense) from the noisy observations of the DME. Figure A-1 shows a block diagram of the implementation of the discrete time Kalman filter. The block labeled K(k) represents the updating of the error covariance matrix based on the present data (the covariance matrix is a statistical matrix which represents the difference between the filtered estimate and the actual state of the system). Therefore, the Kalman filter is a time-varying, optimum statistical estimator which depends on the input and output to alter its filtering process.

The first step was to assume a model for the dynamics of the signal process (aircraft and DME). The aircraft was modeled as a double integrator with acceleration rate (c) as the input and the velocity (range rate, y (t)) as the output (figure A-2). The acceleration rate was assumed to be a random variable. These follow from the underlying assumption that the aircraft is stabilized in an approach configuration. The probability density function F(c) of the acceleration rate (c) which was assumed is shown in figure A-3. In this model, P1 represents a discrete probability that maximum acceleration rate ($\pm A$) will be demanded. P_2 represents the discrete probability that the acceleration rate is not changing. The height of the uniform distribution is:

$$a = (1-2P_1-P_2)/2A$$

The variance of the acceleration rate is:

$$\sigma_c^2 = \frac{A^2}{3}(1+4P_1-P_2)$$

The DME was assumed to present the velocity after adding some noise (n) to it. This measurement noise was assumed to be stationary, additive, of zero mean, and white.

A discrete time model which approximates the assumed dynamic model is shown in figure A-4. The discrete system is described by the following set of equations:

$$\underline{S}(k) = \Phi\underline{S}(k-1)+\underline{w}(k-1)$$
$$\underline{Y}(k) = H\underline{S}(k)+\underline{n}(k)$$

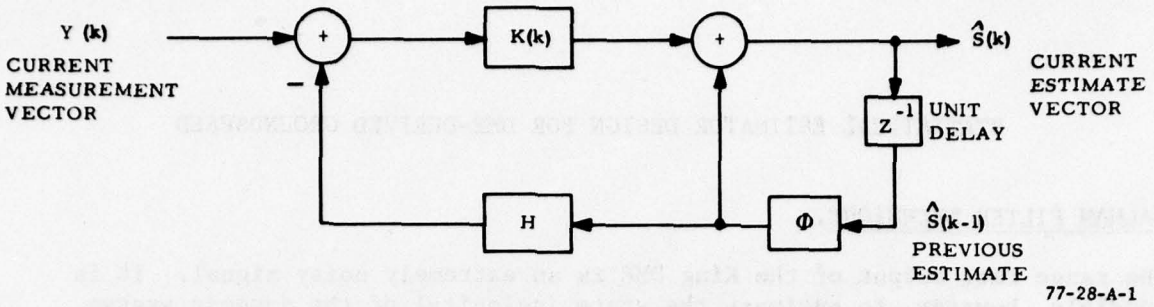

FIGURE A-1. BLOCK DIAGRAM OF KALMAN FILTER IMPLEMENTATION

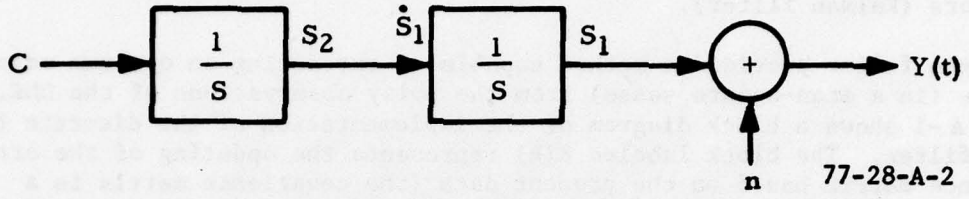

FIGURE A-2. BLOCK DIAGRAM OF AIRCRAFT MODEL

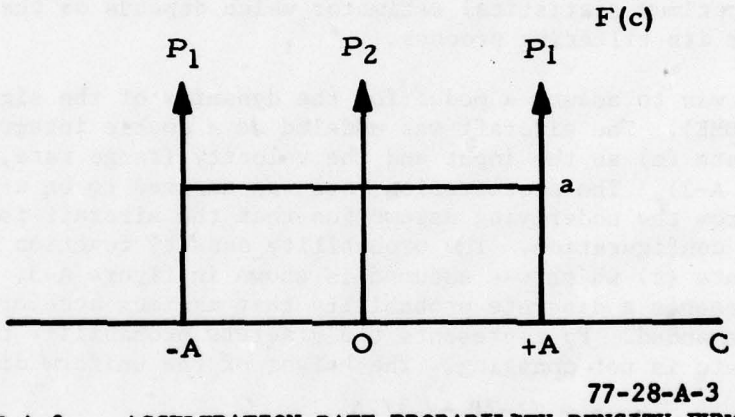

FIGURE A-3. ACCELERATION RATE PROBABILITY DENSITY FUNCTION

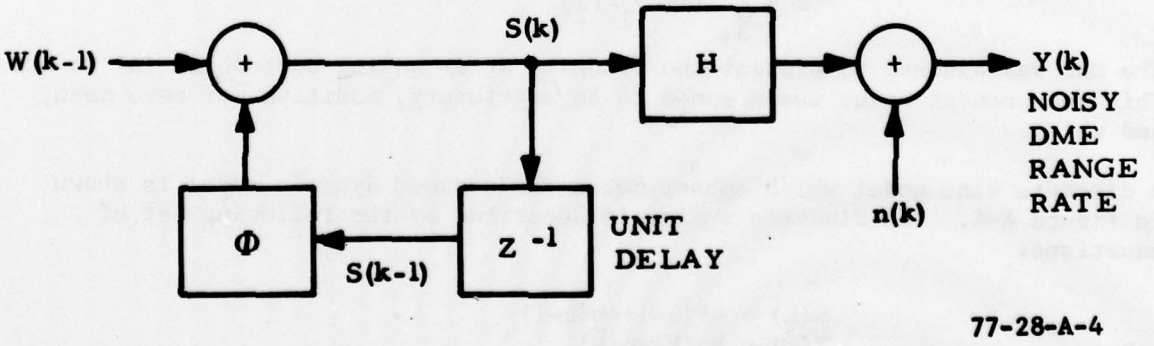

FIGURE A-4. DISCRETE TIME MODEL OF ASSUMED AIRCRAFT SYSTEM

where $\underline{S}$ is the state vector, $\underline{W}$ is the input noise vector, $\underline{Y}$ is the output vector, $\underline{n}$ is the output noise vector, Φ is the state-transition matrix, and H is the measurement matrix.

For the particular model, the values are given below:

$$\Phi = \begin{bmatrix} 1 & T \\ 0 & 1 \end{bmatrix} \quad \underline{S} = \begin{bmatrix} S_1 = \text{Velocity} \\ S_2 = \text{Acceleration} \end{bmatrix}$$

$$H = \begin{bmatrix} 1 & 0 \end{bmatrix} \quad \underline{w} = \begin{bmatrix} 0 \\ w_2 \end{bmatrix} \quad \underline{n} = n_1$$

For the assumed discrete system, the general Kalman algorithm is defined by the following set of matrix equations:

$$K(m) = V(m-1)\, H^T \left[HV(m-1)H^T + R(m) \right]^{-1}$$

$$\hat{\underline{S}}(m) = \underline{S}(m-1) + K(m) \left[Y(m) - H\, \Phi \underline{S}(m-1) \right]$$

$$\tilde{V}(m) = V(m-1) - K(m)\, HV(m-1)$$

$$V(m) = \Phi\, V(m)\, \Phi^T + U(m)$$

$$R(m) = E\left\{ \underline{n}(m)\underline{n}(m)^T \right\} = \sigma_1^2$$

$$U(m) = E\left\{ \underline{w}(m)\, \underline{w}(m)^T \right\} = \begin{bmatrix} 0 & 0 \\ 0 & E\left[w_2^2\right] \end{bmatrix} = \begin{bmatrix} 0 & 0 \\ 0 & \sigma_w^2 \end{bmatrix}$$

where:

K = Kalman gain matrix

V = Predicted covariance matrix

$\tilde{V}$ = Estimate covariance matrix

U = Input noise covariance matrix

R = Output noise covariance matrix

Y = Observation matrix

$\hat{\underline{S}}$ = Optimum estimate vector

E = Expectation operator

All that remains is to define the initial covariance matrices and the initial state vector. The output covariance matrix R was derived empirically from a data tape by comparing raw DME range rate to INS groundspeed and calculating the variance. This was estimated to be 10^4 ft^2/s^2. The input noise to the discrete system is a random acceleration described by:

$$\sigma w = T\, \sigma_c \rightarrow \sigma w^2 = \frac{T^2 A^2}{3} \left(1 + 4P_1 - P_2\right)$$

Therefore, if:

$A = 5\ ft/s^3$
$T = 0.1\ s$
$P_1 = 0.01$
$P_2 = 0.3$
$\sigma_w^2 \approx 0.0625\ ft^2/s^4$

The initial covariance matrix V(0) is defined by:

$$V(0) = E\left\{ \left[S(0) - \hat{S}(0) \right] \left[S(0) - \hat{S}(0) \right]^T \right\}$$

$$V(0) \approx \begin{bmatrix} \sigma_1^2 & \sigma_1^2/T \\ \sigma_1^2/T & \left(\frac{2\sigma_1^2}{T^2} + \sigma_w^2 \right) \end{bmatrix} = \begin{bmatrix} 10^4 & 10^5 \\ 10^5 & 2\times10^6 + 0.0625 \end{bmatrix}$$

The state vector $\underline{S}(0)$ was initialized to the first range rate value for velocity, while the initial acceleration was assumed to be zero. This is not an exact initialization, but it provides a satisfactory starting point.

Since the Collins 860E-3 provides a 30-second low-pass filtered range rate output, the system model for this DME will be slightly different from that of the KDM-7000. The dynamic signal model is shown in figure A-5. In this case, the aircraft is assumed to be an integrator with a random acceleration as the input. The model also includes the filtering imposed by the DME. From this we see that we are going to estimate velocity of the aircraft (S_2) based on observations of filtered range rate (S_1) which also contains a noise term (n). The new state vector $\underline{S}$ becomes:

$$\underline{S} = \begin{bmatrix} S_1 = \text{Filtered range rate} \\ S_2 = \text{Aircraft velocity} \end{bmatrix}$$

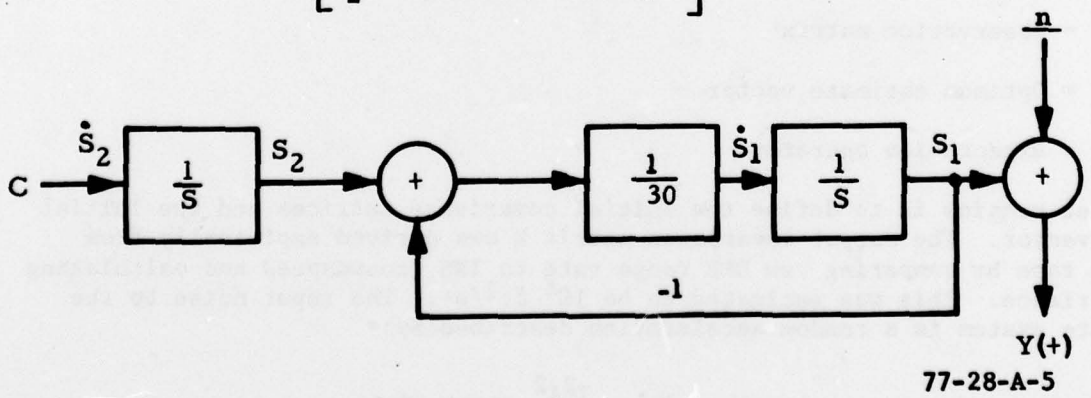

77-28-A-5

FIGURE A-5. SIGNAL DYNAMICS MODEL FOR TOTAL SYSTEM (FOR COLLINS INTERROGATOR)

The state transition matrix 0 for this system for sample period T = 0.1 s is:

$$\Phi = \begin{bmatrix} e^{(-T/30)} & 1-e^{(-T/30)} \\ 0 & 1 \end{bmatrix} = \begin{bmatrix} 0.9967 & 3.328\text{x}10^{-3} \\ 0 & 1 \end{bmatrix}$$

The noise components were assumed to be stationary, additive, white, and of zero mean. For the random input to the discrete system, the assumption was made that 10 ft/s was an approximate 3-sigma value. From this assumption, the variance of the input to the discrete system can be calculated as follows:

$$3\sigma_w = 10 \text{ ft/s}$$

$$\sigma_w = \frac{10}{3} \text{ ft/s}$$

$$\sigma_w^2 = \frac{100}{9} \text{ ft}^2/\text{s}^2, \text{ or } \sigma_w^2 \approx 10 \text{ ft}^2/\text{s}^2$$

A 1-sigma value of 20 ft/s was experimentally determined by trial and error to be a good all-around estimate of the output noise statistics (σn).

The initial covariance matrix in this instance becomes:

$$V(0) = \begin{bmatrix} \sigma_1^2 & \frac{\sigma 1}{1-e^{-T/30}} \\ \frac{\sigma_1}{1-e^{-T/30}} & \frac{2\sigma_1^2}{(1-e^{-T/30})^2} + \sigma w^2 \end{bmatrix}$$

With:

$T = 0.1$ s

$\sigma_1 = 20$ ft/s

$\sigma_w = 10$

Then:

$$V(0) = \begin{bmatrix} 400.00 & 120,200.11 \\ 120,200.11 & 74,240,341.19 \end{bmatrix}$$

This altered system model in no way changes the mechanization of the Kalman filtering algorithm. The filter equations presented during the discussion of the KDM-7000 are directly applicable to the Collins 860E-3 once the appropriate substitutions have been made.

VELOCITY AND ACCELERATION OBSERVATIONS.

By including observations of the longitudinal acceleration, it was possible to greatly improve the performance of the Kalman filter. This entails modifying the discrete system to account for the extra observation. The discrete system block diagram and the filter equations remain the same, although certain matrix and vector quantities must be redefined. The new assignments are made below:

$$H = \begin{bmatrix} 1 & 0 \\ 0 & 1 \end{bmatrix}, \quad \underline{n} = \begin{bmatrix} n_1 = \text{Velocity measurement noise} \\ n_2 = \text{Acceleration measurement noise} \end{bmatrix}$$

$$\underline{w} = \begin{bmatrix} w_1 = \text{Velocity maneuver noise} \\ w_2 = \text{Acceleration maneuver noise} \end{bmatrix}$$

These changes require that the input and output noise covariance matrices (U and R, respectively) be reevaluated.

$$U(m) = E\{w(m)\ w(m)^T\} = 0$$

The U matrix was arbitrarily set to zero. This imposes the condition that the system is not driven by any external noise disturbances.

$$R(m) = E\{\ n(m)\ n(m)^T\}$$

$$R(m) = \begin{bmatrix} \sigma 1^2 & \sigma c^2 \\ \sigma_c^2 & \sigma_2^2 \end{bmatrix}$$

Where:

σ_1^2 = Velocity measurement noise

σ_2^2 = Acceleration measurement noise

σ_C^2 = Cross-correlation measurement noise

The initial covariance matrix V (o) was also modified in accordance with the new design.

$$V(0) = E\left\{\left[\underline{S}(0) - \hat{\underline{S}}(0)\right]\ \left[\underline{S}(0) - \hat{\underline{S}}(0)\right]^T\right\}$$

The best assumption which could be made here is that the best a priori estimate S(0) will be the initial measurement.

$$\hat{\underline{S}}(0) = H\underline{S}(0) + \underline{n}(0)$$

$$\text{Since } H = \begin{bmatrix} 1 & 0 \\ 0 & 1 \end{bmatrix}, \quad \hat{\underline{S}}(0) = \underline{S}(0) + \underline{n}(0)$$

and therefore:

$$V(0) = E\left\{-\underline{n}(0)\left[-\underline{n}(0)^T\right]\right\} = E\left\{\underline{n}(0)\ \underline{n}(0)^T\right\}$$

$$E\left\{\underline{n}(0)\ n(0)^T\right\} = E\left\{n(m)n(m)^T\right\}$$

Hence the initial covariance matrix was set equal to the output noise covariance matrix. V(0)=R(m)

From this point on, the initialization and implementation of the Kalman filter for the KDM-7000 is straightforward. The velocity measurement covariance σ_1^2 is the same as before, 10^4 $(ft/s)^2$. The correlation terms of R(M) were arbitrarily set equal to zero. The acceleration measurement covariance σ_2^2 was experimentally determined (by trial and error) to be $10^{-4}(ft/s)^2$. This was the value which provided the best filter performance.

Hence:

$$V(0) = R(m) = \begin{bmatrix} 10^4 & 0 \\ 0 & 10^{-4} \end{bmatrix}$$

The initial velocity was set equal to the first range rate measurement $Y_1(0)$, and the initial acceleration was arbitrarily set equal to zero.

$$\underline{S}(0) = \begin{bmatrix} Y_1(0) \\ 0 \end{bmatrix}$$

The Collins 860E-3 may be handled in an identical manner if the effect of the 30-second low-pass filter is treated as measurement noise. The implementation and assumptions are identical to those made in the case of the KDM-7000. Only the values of σ_1^2 and σ_2^2 are different. The velocity measurement covariance σ_1^2 used for the Collins 860E-3 was 400 ft/s^2. The acceleration covariance which provided the best performance in this case was 0.001 ft/s^2.

$$V(0) = R(m) = \begin{bmatrix} 400 & 0 \\ 0 & .001 \end{bmatrix}$$

Due to the extremely noisy nature of the KDM-7000 range rate output (figure 25), it was necessary to place a limiter on the input to the Kalman filter. This limited the velocity to a range of 125 to 325 ft/s. An identical limiter was utilized with the Collins 860E-3; however, it was not necessary to do so. The limiter was used for all of the Kalman filter results presented in the report. The limiter eliminated gross outliers and reduced the noise on the output of the Kalman filter.

When the observation of acceleration was included, bias errors were encountered which were not reduced by the Kalman filter. Since the Kalman filter is based on optimizing mean square error, this is not overly surprising. The pitch-compensated longitudinal acceleration term was high-pass filtered to wash out these biases. The high-pass filter was actually time-varying in nature. This was accomplished by incrementing the filter time constant from an initial value to some final value. This technique hastened the washout and still provided adequate bandwidth once the filter was in the steady-state condition. The filter for the KDM-7000 was initialized to a 1-second time constant and allowed to increment up to a 60-second time constant. In the case of the Collins 860E-3, we found that we had to initialize at a 30-second time constant and increment up to a 60-second time constant. In each case, the time constant was incremented at the rate of 0.1 second per sample period. This provided a much better covariance of the output of the Kalman filter. We also found a need to premultiply the filtered acceleration by a gain factor before entering the Kalman filter. The KDM-7000 required a gain of 1.5, while the 860E-3 required a gain of 1.8 to provide a useful result.